Neutron-hole distributions in ^{111,115,119}Sn as observed in the (^{3}He,α) reaction

E. Gerlic, G. Berrier-Ronsin, G. Duhamel, S. Galès, E. Hourani,* H. Langevin-Joliot, M. Vergnes, and J. Van de Wiele

Institut de Physique Nucléaire, BP n°1, 91406 Orsay, France

(Received 27 June 1979)

The energy spectra of residual ^{111,115,119}Sn nuclei have been studied with 38 keV resolution, up to excitation energies of the order of 16 MeV, using the (^{3}He,α) reaction at 39 MeV. Complete angular distributions have been obtained for the ^{116}Sn(^{3}He,α)^{115}Sn reaction; two angles were measured for the other isotopes. Several new levels or groups are observed up to ~ 3.5 MeV in the three isotopes, owing to the momentum matching conditions. Spectroscopic factors are determined for all observed levels up to 3.71 MeV in ^{115}Sn and for the low-lying strongly populated levels with known J^π in ^{111,119}Sn. The fragmentation of the $l = 4$, 5 valence hole strengths and the excitation of levels with anomalous spins and parities in the intermediate energy region in ^{115}Sn are discussed in terms of weak-coupling and two-step coupled channels calculations. The fine structure previously reported for the $1g_{9/2}$ hole orbital in ^{115}Sn is clearly confirmed and enhanced in the present experiment. The fragmentation of this orbital is observed for the first time in ^{111}Sn, between 3.4 and 5.2 MeV and in ^{119}Sn, though to a lesser extent, between 3.8 and 6.5 MeV. In the fine structure region the $1g_{9/2}$ hole strength is found to decrease from 62% to 43% and 28% in ^{111}Sn, ^{115}Sn, and ^{119}Sn, respectively; theoretical calculations do not explain these experimental strengths and fragmentations. The first $9/2^+$, $1/2^-$, $3/2^-$ isobaric analog states are identified in ^{111}Sn. Previously unreported, weakly populated isobaric analog states are also found in ^{115}Sn and ^{119}Sn. The energies and widths are measured. The spectroscopic factors and isospin splitting of these states are discussed in the framework of the Lane coupled-channels formalism for the neutron form factor.

[NUCLEAR REACTIONS ^{112,116,120}Sn(^{3}He, α) $E = 39$ MeV; measured $\sigma(E_\alpha, \theta)$ ^{111,115,119}Sn deduced levels, E_x, l, $(J)^\pi$, C^2S; zero-range DWBA and two-step process analysis; inner shells and isobaric analog states analysis: enriched targets, magnetic spectrometer.

NUCLEAR STRUCTURE unified model calculations.]

I. INTRODUCTION

In the last few years, neutron pickup experiments on the tin isotopes have been carried out using the reactions (d, t) at 23 (Ref. 1 and 2) and 52 MeV,[3] (p,d) at 20 (Ref. 4) and 52 MeV,[5] (^{3}He, α) at 89,[5] 120,[6] and 205 MeV.[7] With the exception of Ref. 4, these studies were concentrated on deeply bound hole states and in some cases on their corresponding isobaric analog states (IAS). The (^{3}He, α) studies were performed with rather poor energy resolution (190–400 keV). The recent high resolution study of the ^{116}Sn(d, t) ^{115}Sn reaction at 23 MeV (Ref. 1) demonstrated an underlying fine structure between 4 and 6 MeV excitation energy, with both $l = 4$ and $l = 1$ inner-hole components. This reaction also proved useful for the determination of a number of transitions with small l values at lower excitation energy.[2]

We present in this paper a rather extensive study of the (^{3}He, α) reaction at 39 MeV incident energy on ^{116}Sn and a cursory investigation at two angles of this reaction on ^{112}Sn and ^{120}Sn. The selectivity of the (^{3}He, α) reaction for high angular momentum, together with the adequate energy resolution (38 keV), were used in order to investigate the fragmentation of $1g_{7/2}$ and $1h_{11/2}$ valence orbitals as well as that of the $1g_{9/2}$ inner orbital. The spectra of the residual nuclei were investigated up to ~16 MeV excitation energy.

After a short description of the experimental procedure (Sec. II), we present in Sec. III the analysis of the data, involving zero-range one-step DWBA calculations. Two-step processes, in the framework of the weak-coupling model, will be considered in the discussion of neutron-hole states fragmentation at intermediate excitation energies, i.e., from ~1 up to ~3.7 MeV (Sec. IV). Rather sparse spectroscopic information exists in that region, especially in the case of ^{111}Sn. In Sec. V the observed fragmentation of the $1g_{9/2}$, $T_<$ inner-hole strength in the Sn isotopes around 5 MeV excitation energy will be discussed. In Sec. VI, data and analysis of the $T_>$ ($1g_{9/2}$, $2p_{3/2}$, $2p_{1/2}$, and $1f_{5/2}$) inner-hole components will be presented.

II. EXPERIMENTAL PROCEDURE

The ^{112,116,120}Sn(^{3}He, α) reactions were studied at 39 MeV incident energy using the ^{3}He beam de-

livered by the Orsay MP Tandem accelerator. The outgoing α particles were detected in eight position sensitive detectors (PSD) in the focal plane of the split pole magnetic spectrometer. The solid angle of the spectrometer was 1.7 msr. The targets consisted of self-supporting metal foils of ^{112}Sn (420 μg/cm^2, 83.64% enrichment), ^{116}Sn (290 μg/cm^2, 95.74% enrichment), and ^{120}Sn (380 μg/cm^2, 98.4% enrichment) prepared by vacuum evaporation. An overall energy resolution of 38 keV was achieved. The α particle spectra obtained for the three targets are presented in Figs. 1 and 2 for the low-lying states (E_x<4 MeV). The excitation energy range from ~3 to ~16 MeV, where the $T_<$ and $T_>$ components of inner-hole states are observed, is displayed for the three isotopes in Fig. 3.

The absolute cross sections were determined by measuring the thicknesses of the targets using an α gauge. The beam current was measured in a Faraday cup. The error in the absolute cross-section scales is estimated to be of the order of ±13%. The excitation energies of the observed levels have been determined from calibration of the PSD using both a Th C α source and reaction α particles. The uncertainties on the excitation energies are estimated to be of the order of ±8 keV for strong transitions up to 6 MeV and about ±15 keV for weaker or complex groups for E_x>6 MeV. Angular distributions have been measured from 4° to 22°, typically by 2° steps, in the case of the ^{116}Sn(^{3}He, α) ^{115}Sn reaction. The spectra of the ^{112}Sn(^{3}He, α) ^{111}Sn and ^{120}Sn(^{3}He, α) ^{119}Sn reactions have been measured at θ_{lab} = 4° and 12° for comparison. The most forward angles could only be measured, with reasonable beam intensity, by removing the defining slits at the entrance of the scattering chamber.

In Figs. 1 and 2 one can notice that, above ~2 MeV, the spectrum no longer consists of well separated levels. Peaks or groups of peaks are, however, clearly identified at most angles and angular distributions could be obtained for ^{115}Sn by dividing the spectra into adjacent slices carefully chosen in order to be consistent with our previous (d, t) work. The experimental angular distributions, obtained using such a procedure, were found to be rather simple and could in most cases be fitted by a dominant l transfer, owing to the high selectivity for large l values of the (^{3}He, α) reaction.

III. DISTORTED-WAVES ANALYSIS, OPTICAL POTENTIAL PARAMETERS

The experimental angular distributions obtained in the study of the ^{116}Sn(^{3}He, α) ^{115}Sn reaction were analyzed first in the framework of the distorted-wave Born approximation (DWBA) theory of direct

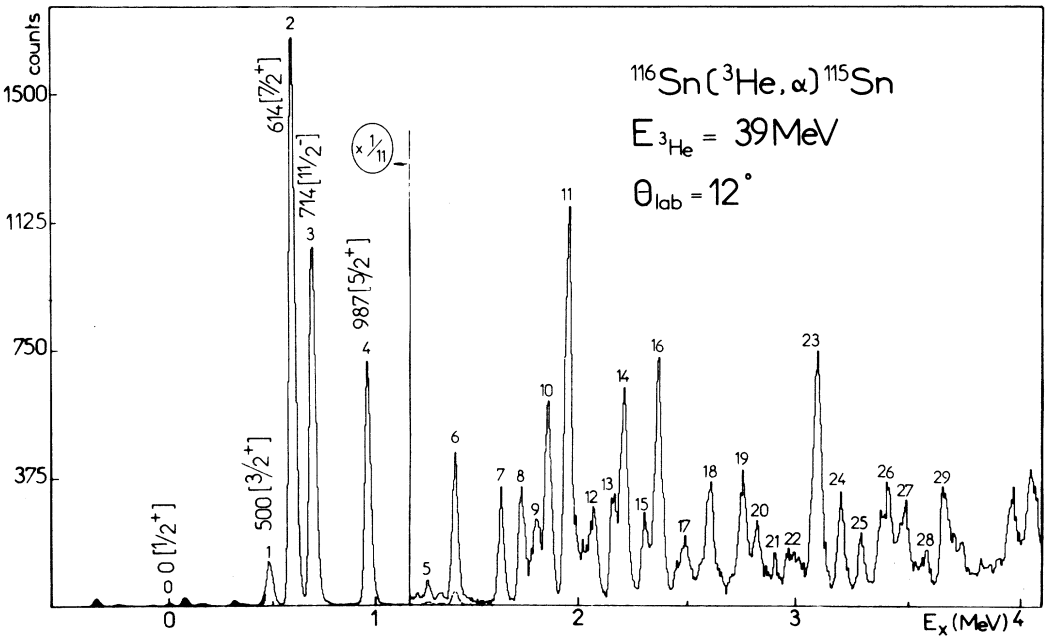

FIG. 1. The α energy spectrum from the ^{116}Sn(^{3}He, α)^{115}Sn reaction at 12° laboratory. The numbers on the top of the peaks refer to ^{115}Sn levels and are listed in Table II. Two successive exposures at different magnetic fields were necessary in order to observe the complete range of excitation energy. The spectrum shown was obtained by combining two successive spectra accumulated at 12°, which had an overlap in excitation energy of about 200 keV.

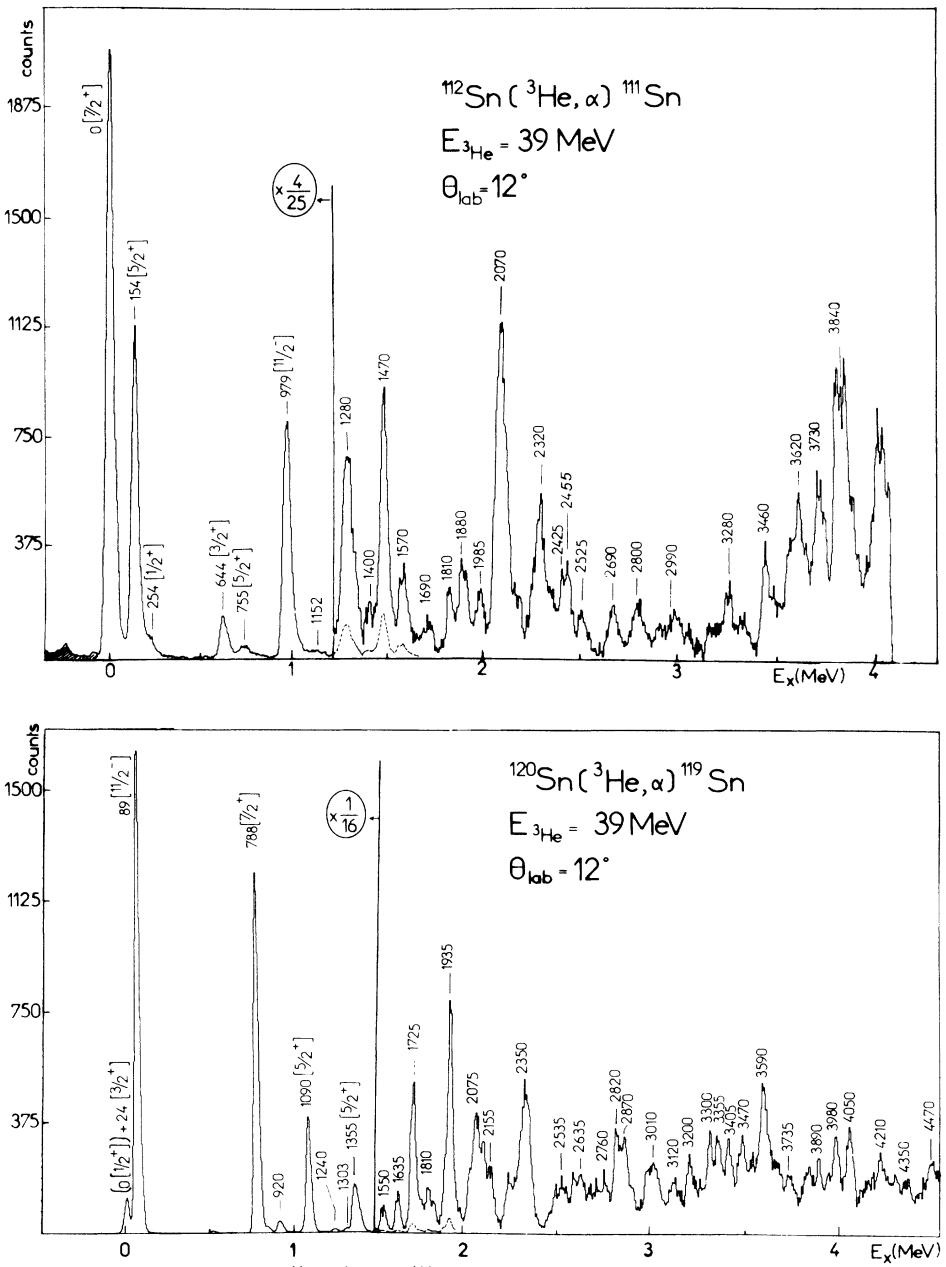

FIG. 2. The α energy spectra from the ^{112}Sn(^{3}He, α)^{111}Sn reaction (top part) and the ^{120}Sn(^{3}He, α)^{119}Sn reaction (bottom part). The low-lying levels in ^{111,119}Sn are labeled by their excitation energies, spins, and parities. Only the excitation energies are reported for levels above ~1.2 MeV in both isotopes. The procedure used to obtain these spectra is the same as described in the caption of Fig. 1.

reactions. The calculations of the theoretical curves were made using the code DWUCK [8] with the zero-range, local approximation (ZRL).

A number of different sets of ^{3}He and α optical potentials (deep families), taken from the compilation of Perey *et al.*[9] and/or from some more recent elastic scattering and transfer reaction studies,[10] were used in order to reproduce the strongest transitions at E_x = 614 keV, $\frac{7}{2}^+ - E_x$ = 714 keV, $\frac{11}{2}^-$, and E_x = 985 keV, $\frac{5}{2}^+$ in ^{115}Sn. No significant differences were observed in the shapes of the angular distributions or in the resulting relative cross sections for different l values. However, depending on the choice of the optical parameters, the absolute cross sections were found to show differences of the order of ±15% for a given level.

Table I gives the adopted sets of parameters[10,11] for the ^{3}He and α channels. The same potentials

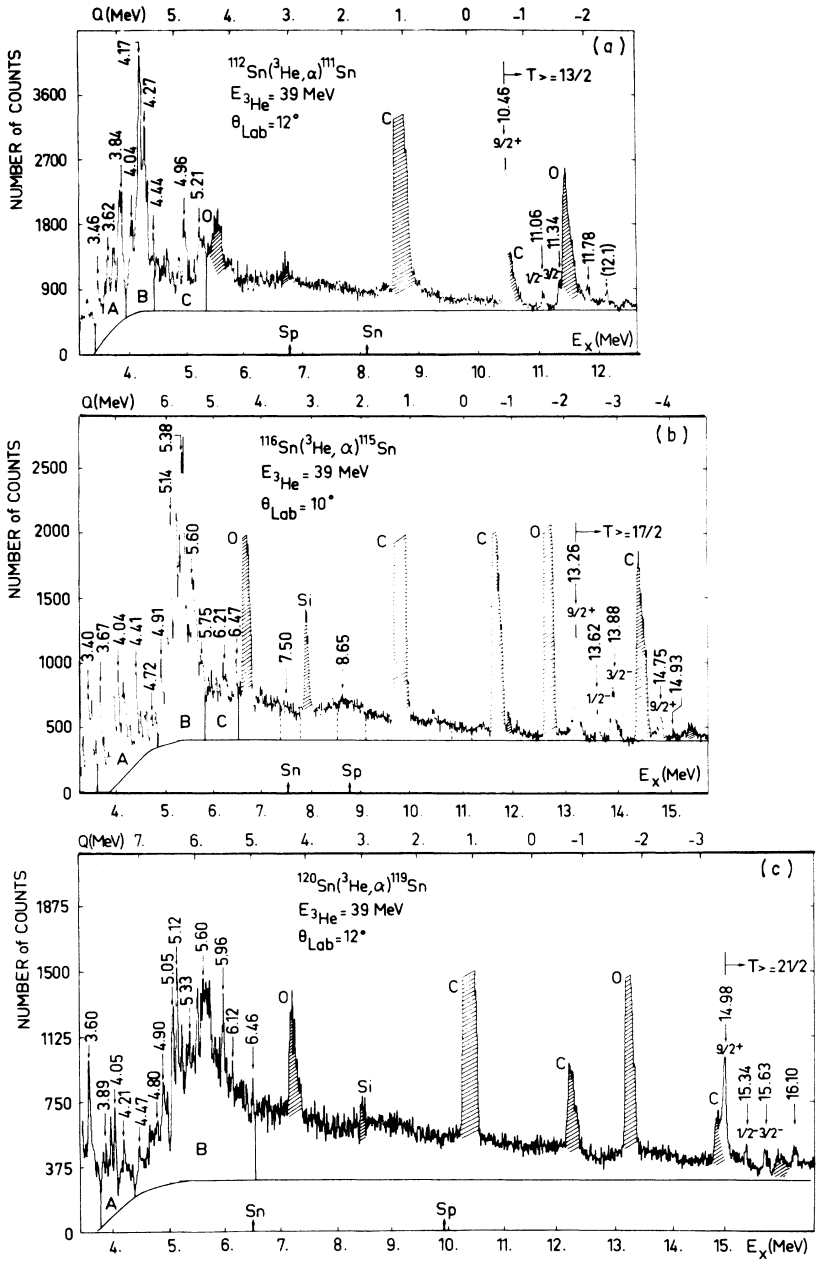

FIG. 3. (a) The α energy spectrum from the ^{112}Sn(^{3}He, α)^{111}Sn reaction at 12° laboratory. The excitation energy range displayed (3.0 to 13 MeV) permits the observation of both $T_<$ and $T_>$ components of inner-hole states in ^{111}Sn. The solid horizontal line going from ~3 to 13 MeV represents our assumption about the background. The limits of the regions A, B, and C, where mostly concentrated is the $1g_{9/2}$ inner-hole strength, are indicated by vertical solid lines. In the horizontal scale, the binding energies of a proton (S_p) and of a neutron (S_n) are noted. The procedure indicated in the caption of Fig. 1 was used for the eight PSD in order to build the spectrum presented here. (b) Same as (a) for the ^{116}Sn(^{3}He, α)^{115}Sn reaction ($3.5 \leq E_x \leq 16$ MeV). (c) Same as (a) for the ^{120}Sn(^{3}He, α)^{119}Sn reaction ($3.5 \leq E_x \leq 16$ MeV).

were used to extract spectroscopic factors for the well known low-lying levels in ^{111,119}Sn. The normalization constant N was taken as equal to 23 in the whole analysis.

A more refined analysis, taking into account two-step processes for some levels in ^{115}Sn or using a Lane form factor for $T_>$ states, will be discussed in Secs. IV and VI.

TABLE I. Optical parameters used in the analysis of the ^{112,116,120}Sn(^{3}He, α)^{111,115,119}Sn reactions at 39 MeV.

	V (MeV)	r (fm)	a (fm)	W (MeV)	r_i (fm)	a_i (fm)	λ	Ref.
^{3}He	176.2	1.24	0.67	32.8	1.38	0.84		a
α	206	1.41	0.52	25.8	1.41	0.52		b
n	adjusted	1.25	0.65				25	

[a] Reference 11. [b] Reference 10.

IV. FRAGMENTATION IN THE LOW AND INTERMEDIATE ENERGY REGION ($0 < E_x < \sim 3.7$ MeV)

A. DWBA analysis of the ^{116}Sn(^{3}He, α)^{115}Sn reaction

The measured cross sections for the first low-lying levels ($\frac{1}{2}^+, \frac{3}{2}^+, \frac{7}{2}^+, \frac{11}{2}^-, \frac{5}{2}^+$) in ^{115}Sn clearly demonstrate the selectivity of this reaction for high spin states (see Figs. 1 and 4). Moreover, the transitions $l=0$ to the $E_x = 0.0$ and 1964 keV levels, strong in the (d, t) spectrum,[2] are barely visible in the (^{3}He, α) spectrum (see Figs. 1 and 4 and Table II).

Above 2.6 MeV excitation energy in ^{115}Sn the observed cross section remains large in the (^{3}He, α) spectrum (see Fig. 1) while in the (d, t) spectrum the cross section is much smaller in the same excitation energy range. This observation suggests that high l components are present in this part of the spectrum.

The experimental angular distributions are displayed in Figs. 4 and 5. As expected for the (^{3}He, α) reaction, they are not very characteristic of the transferred angular momentum, especially for two transfers differing by only one unit of l ($l=4$ or 5, for example). However, a careful comparison between the experimental data and theoretical DWBA curves allows in most cases unique l assignment for the observed levels in ^{115}Sn. In addition, comparison has been made with the ^{116}Sn$(d, t)^{115}$Sn results in order to clarify any ambiguous assignment due to the contribution of two different l values within the same complex peak. The deduced spectroscopic information is presented in Table II together with the C^2S values from the ^{116}Sn$(d, t)^{115}$Sn study.[2] The main characteristics of the intermed-

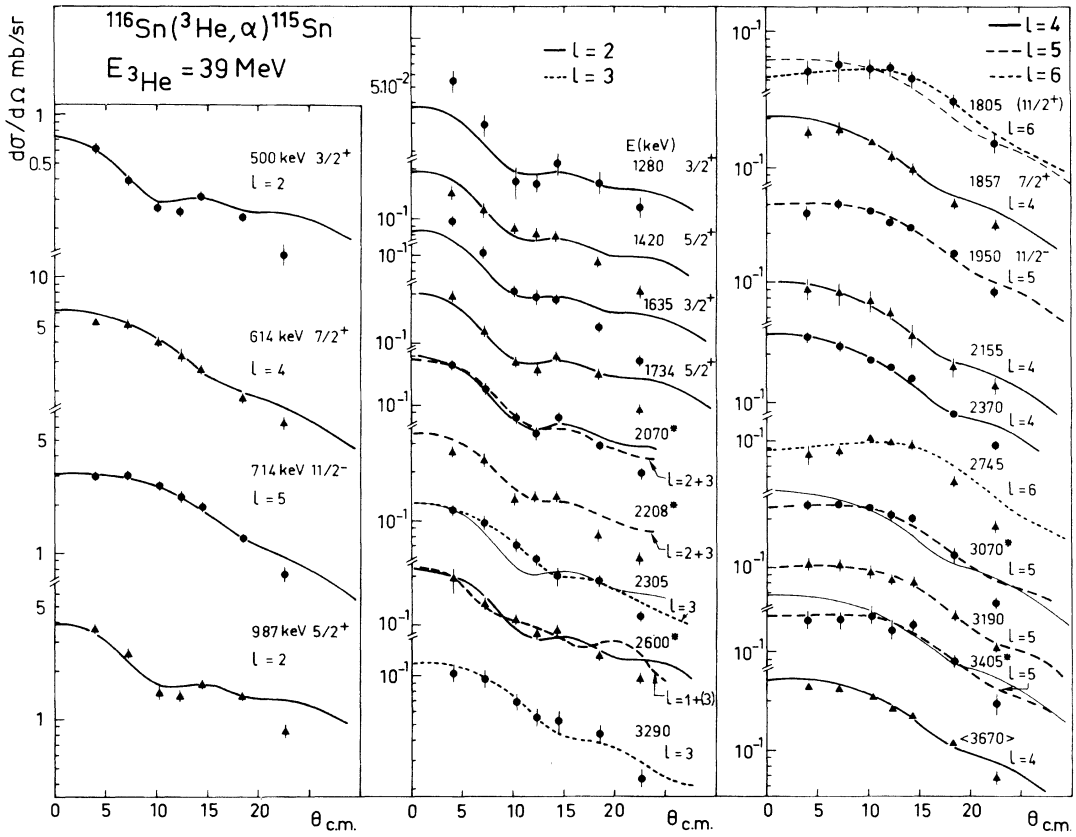

FIG. 4. Angular distributions from the ^{116}Sn(^{3}He, α)^{115}Sn reaction to discrete levels with $l=2$, 3, 4, 5, and 6 angular momentum transfers. The curves show the DWBA predictions. Each final state is identified by its excitation energy in ^{115}Sn. Vertical bars are statistical errors.

TABLE II. ^{116}Sn(^{3}He, α)^{115}Sn—39 MeV.

$E_x(d,t)$ [a] (keV)	Present work n^0=pic	Present work E_x (keV)	Present work l	Present work $J\pi$ [b]	Present work C^2S this work	C^2S [a] (d,t)
0	0	0	...	$\frac{1}{2}^+$	...	0.7
500	1	500	2	$\frac{3}{2}^+$	1.2	0.9
614	2	614	4	$\frac{7}{2}^+$	7.5	5.9
714	3	714	5	$\frac{11}{2}^-$	2.03	1.6
987	4	987	2	$\frac{5}{2}^+$	4.7	4.0
1282	5	1280	2	$\frac{3}{2}^+$	0.055	0.1
1420	6	1420	2	$\frac{5}{2}^+$	0.205	0.074
1639*	7	1635	2	$\frac{3}{2}^+$	0.17	0.13
1734	8	1734	2	$\frac{5}{2}^+$	0.18	0.15
...	9	1805	6	$(\frac{11}{2}^+)$	(0.14)	...
1856	10	1857	4	$\frac{7}{2}^+$	0.2	0.33
1944	11	1950	5	$(\frac{11}{2})^-$	0.22	(0.077)
1964	...	...	...	$\frac{1}{2}^+$	...	0.14
		(1995)	(2)	...	...	...
2061*	12	2070*	2 + (3)	$\frac{5}{2}^+, (\frac{3}{2}^+)$	(0.08) ⟷	0.08
2081				$(\frac{5}{2}^-, \frac{7}{2}^-)$	(0.1, 0.07)	
2155	13	2155	4	$(\frac{7}{2}, \frac{9}{2})^+$	(0.12, 0.07)	...
2206*	14	2208*	2 + (3)	$\frac{3}{2}^+, (\frac{5}{2}^+)$	(0.13) ⟷	0.13
				$(\frac{5}{2}^-, \frac{7}{2}^-)$	(0.22, 0.15)	
2302	15	2305	3	$\frac{5}{2}^-, \frac{7}{2}^-$	0.19, 0.13	(0.1)
2355	16	2370	(2)	$(\frac{5}{2}^+)$	(0.05) ⟷	0.05
2371			4	$(\frac{7}{2}, \frac{9}{2})^+$	0.26, 0.15	0.35
		2450	(1)			
2489	17	2487*	4	$(\frac{7}{2}^+)$	0.11	
2520				$(\frac{5}{2}^+)$	...	(0.014)

$E_x(d,t)$ [a] (keV)	Present work (*Continued*) n^0=pic	Present work (*Continued*) E_x (keV)	Present work (*Continued*) l	Present work (*Continued*) $J\pi$ [b]	Present work (*Continued*) C^2S this work	C^2S [a] (d,t)
		(2560)	(1)	$(\frac{1}{2}^-)$	(0.15)	
2593	18	2600*	1 + ≥3	$(\frac{1}{2}^-)$ + $\geq \frac{5}{2}^-$	(0.32)	0.16
		2650				
		(2700)				
2735	19	2745	(6)	$(\frac{13}{2}^+)$		
2805	20	2807*	2 + ≥3	$(\frac{5}{2}^+)$ + $\geq \frac{5}{2}^-$	(0.05) ⟷ ≤0.1	0.05
2855		(2860)	(6)			
	21	2890	5	$(\frac{11}{2}^-)$	0.027	
2930						
2950*		2950	(2)	$(\frac{5}{2}^+)$	0.04	0.03
2980	22	2985	5, (4)	$(\frac{11}{2}^-)$	0.03	
3000				$(\frac{5}{2}^+)$		0.026
3060	23	3070*	(4) + 5	$(\frac{9}{2}^+)$		0.032
3080				$(\frac{11}{2}^-)$	0.2	
3190	24	3190	5	$(\frac{11}{2}^-)$	0.08	
3300	25	3290	3	$\frac{7}{2}^-, \frac{5}{2}^-$	0.11, 0.16	
	26	3405*	5			
3500	27	3490*	5, 4	$(\frac{11}{2}^-, \frac{9}{2}^+)$	(0.09, 0.1)	(−, 0.083)
	28	3590*	4, (5)	$(\frac{9}{2}^+, \frac{11}{2}^-)$	<0.07	
3665	29	3.67	4	$(\frac{9}{2}^+)$	0.2	0.17
3690						
3710		3.73		$(\frac{9}{2}^+)$		

[a] See Ref. 2. Only the levels having an energy correspondence with those observed in the present (^{3}He, α) work are given in column 1. The asterisk refers to a broad peak, possibly a doublet.

[b] Known values or/and values proposed and used in the present DWBA calculations. The double headed arrow means that C^2S value of (d,t) has been taken as a reference.

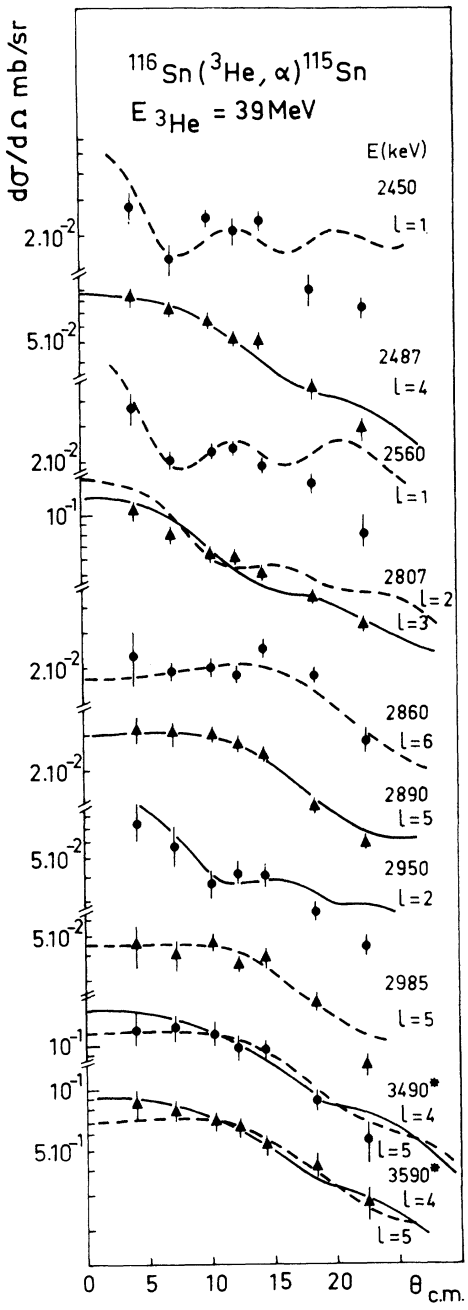

FIG. 5. Angular distributions from the ^{116}Sn(^{3}He, α)^{115}Sn reaction for weaker and complex structures observed in the intermediate energy range $1 \leq E_x \leq 3.5$ MeV. The curves are DWBA predictions for different l values. Vertical bars are statistical errors.

iate energy region ($E_x = 1$ to 3.7 MeV) are the following.

(i) The states observed for the first time in the (d, t) experiment[2] with an angular momentum $l \geq 3$ are clearly enhanced in the (^{3}He, α) spectrum: The 1950 keV state, which dominates this part of the spectrum, has a definite $l = 5$ angular momentum transfer, suggesting $J^\pi = \frac{11}{2}^-$ from shell model considerations. The 2155, 2370, and 3670 keV states have angular distributions in good agreement with an $l = 4$ transfer, leading to spin and parity assignments $J^\pi = \frac{7}{2}^+$ or $\frac{9}{2}^+$. The 2305 and 3290 keV states have an $l = 3$ angular distribution, suggesting spin and parities $J^\pi = \frac{5}{2}^-$ or $\frac{7}{2}^-$.

(ii) In addition, new states are observed in this (^{3}He, α) experiment: The 1805 keV state has an angular distribution nicely reproduced by an $l = 6$ transfer. The peaks or groups of peaks located respectively at 3070, 3190, 3405, and possibly 3490 keV are populated through an $l = 5$ transfer. An $l = 4$ component may also contribute to the complex 3070 keV peak, as suggested by the (d, t) analysis. A number of weaker transitions are identified as $l = 4$ ($E_x = 2487$ and 3590 keV), $l = 5$ ($E_x = 2890$ and 2985 keV), $l = 6$ ($E_x = 2860$ keV); the rather strong 2745 keV transition might also be $l = 6$.

(iii) We would like to stress that probable $l = 3$ transitions are observed at ~2080 and 2208 keV. In both the (d, t) and (^{3}He, α) studies, these levels are observed as complex peaks and have dominant $l = 2$ contributions in their angular distributions. However, the extracted C^2S values assuming a simple $l = 2$ transfer are much larger in the (^{3}He, α) study than in the (d, t) work. An attempt was made to explain the discrepancies by introducing small contributions from an $l = 3$ angular momentum transfer in the DWBA analysis. The resulting fits to the experimental data assuming $l = 2 + 3$ mixing are presented in Fig. 4 and the deduced C^2S values are listed in Table II. These $l = 3$ contributions are in agreement with the spin assignments $(\frac{5}{2}, \frac{7}{2})$ for the level at 2207 keV in Madueme's work[12] and with the recent results of Fleming *et al.*[13] in their study of the ^{115}Sn$(p, p')^{115}$Sn reaction. In this last experiment, strongly excited levels at $E_x = 2090$, 2200, and 2310 keV are assigned $J^\pi = \frac{5}{2}^-$ or $\frac{7}{2}^-$.

(iv) Finally, we note the rather large discrepancy observed between the spectroscopic factors deduced from the (^{3}He, α) and (d, t) reactions, for the unambiguous $l = 2$ transitions populating the levels at $E_x = 1280$ and 1420 keV (see Table II). The behavior of the two states, in the two experiments, is obviously different, leading to the observed differences in the C^2S values. As was already pointed out in the previous (d, t) work,[2] these levels are, respectively, the second $J^\pi = \frac{3}{2}^+$ and $J^\pi = \frac{5}{2}^+$ levels of ^{115}Sn and are predicted to have wave functions containing very large $|3s_{1/2} \otimes 2^+\rangle$ collective components. This is confirmed by the strong excitation of these levels in the (p, p') experiment of Flemming.[13] The observed anomalies are therefore very probably due to two-step processes in both reac-

tions.

In summary, the intermediate energy region in ^{115}Sn ($E_x = 1$ to 3.7 MeV) is dominated by a large number of transitions with $l = 3$, 4, 5, and 6 transfers. In the framework of a simple shell model the observation of such $l = 6$ ($\frac{11}{2}^+$, $\frac{13}{2}^+$) as well as $l = 3$ ($\frac{5}{2}^-$, $\frac{7}{2}^-$) states at so low an excitation energy is clearly unexpected. It is also quite difficult to explain the presence of "anomalous" negative parity states populated through an $l = 1$ transfer ($\frac{1}{2}^-$, $\frac{3}{2}^-$), strongly enhanced in the (d, t) experiment.[2] The observation, at low excitation energy, of these "anomalous l" states populated with small but non-negligible spectroscopic factors ($C^2S < 0.2$) is an indication of the need for a refined description of the low-lying levels of ^{115}Sn. The introduction of a weak-coupling model, already proposed in our previous (d, t) study to explain the fragmentation of the $l = 2$, ($2d_{3/2}$ and $2d_{5/2}$) subshells in ^{115}Sn, could give a quantitative explanation to the fragmentation observed in this excitation energy region for the $l > 2$ orbitals in ^{115}Sn.

B. Weak-coupling model for ^{115}Sn

In order to explain the population of "anomalous states" in the intermediate excitation energy region, an unified model calculation has been performed. The quasihole neutron configurations of valence as well as of inner orbitals are coupled to the quadrupole (2^+) and octupole (3^-) vibration modes of the doubly even ^{116}Sn nucleus. The required formulas involved in these calculations are rather standard and have been reported in detail, for example, in Ref. 14. The computer code QUPHONON written by K. Heyde,[15] was used to obtain the wave functions of the ^{115}Sn levels based on this model. All combinations up to three quadrupole and two octupole phonons, with experimental phonon energies $\hbar\omega_2 = 1.27$ MeV and $\hbar\omega_3 = 2.27$ MeV, are introduced in the calculations. The quasihole neutron valence orbitals outside the $N = 50$ core ($3s_{1/2}$, $2d_{5/2}$, $2d_{3/2}$, $1g_{7/2}$, $1h_{11/2}$) as well as inner neutron-hole orbitals ($1g_{9/2}$, $2p_{1/2}$, $2p_{3/2}$, $1f_{5/2}$, $1f_{7/2}$) were also introduced in the calculations. The valence occupation probabilities V_j^2 were taken as the mean values between those extracted from previous neutron pickup data[2,3,16] on ^{116}Sn and those from the present (^{3}He, α) data. This procedure seems to relax somewhat the dependence on momentum mismatch effects in a particular reaction and on reaction mechanisms. The different allowed combinations for a given J^π value, up to an excitation energy of $E_x = 12$ MeV, are taken into account to prevent any effect due to a limited configuration space in the relevant excitation energy region. The coupling strength $\xi_\lambda = \langle r\partial V/\partial r\rangle \beta_\lambda 1/\hbar\omega_\lambda\sqrt{\pi}$ is estimated from inelastic scattering or Coulomb excitation measurements, using the currently adopted value of 40–50 MeV for the expression $\langle r\partial V/\partial r\rangle$. The values of ξ_λ as well as the quasihole energies were considered to some extent as parameters in the analysis in order to reproduce the level sequence of the first well known low-lying levels in ^{115}Sn, where the lowest level of each spin is known to carry the main part (>75%) of the corresponding measured strength. The largest deviation (465 keV) between any nlj quasihole energy and the experimental excitation energy of the corresponding lowest J^π excited state is found for $2d_{5/2}$, showing a relatively larger fragmentation of this orbital. The resulting values of ξ_2 and ξ_3, quasihole energies E_{qh} and occupation probabilities V_j^2, are reported in Table III. The agreement is rather good as shown in Fig. 6. The large spectroscopic factors of the first five levels below 1 MeV are well reproduced by the unified model. These theoretical values are defined as $C^2S = (2j+1)\, V_j^2 C_j^2 0^+$, where $C_j 0^+$ is the amplitude of the l_j quasihole coupled to the 0^+ ground-state core. The first level of each spin has a rather pure single hole character ($C_j 0^+ \geq 0.92$, except for the $\frac{5}{2}^+_1$ level where $C_j 0^+ = 0.84$), leading to very small predicted C^2S values for all the other states located above 1 MeV, in agreement with the general trend experimentally observed.

The introduction of five inner orbitals extends our previous unified model calculation in ^{115}Sn, where only the $1g_{9/2}$ inner orbital was considered in addition to the six valence orbitals. Thus the present calculation predicts, in particular, that small but significant fractions of the $2p$ and $1f$

TABLE III. Input parameters for QUPHONON code (weak-coupling calculations in ^{115}Sn).

	nl	j	E_{qh} (MeV)	V_j^2
Valence shells	$3s$	$\frac{1}{2}$	0.050	0.42
	$2d$	$\frac{3}{2}$	0.600	0.37
	$1g$	$\frac{7}{2}$	0.850	0.89
	$1h$	$\frac{11}{2}$	0.900	0.18
	$2d$	$\frac{5}{2}$	1.450	0.80
Inner shells	$1g$	$\frac{9}{2}$	6.2	1.0
	$2p$	$\frac{3}{2}$	6.5	1.0
	$2p$	$\frac{1}{2}$	7.5	1.0
	$1f$	$\frac{5}{2}$	8.5	1.0
	$1f$	$\frac{7}{2}$	9.5	1.0
$\hbar\omega_2 = 1.27$ MeV; $\xi_2 = 2.0$				
$\hbar\omega_3 = 2.27$ MeV; $\xi_3 = 1.0$				

strengths are concentrated on a few relatively low-lying (2 to 3 MeV) levels, in agreement with the (d, t) observations and with the predictions of Ref. 17. We wish to emphasize that these calculations predict large l transitions, populating positive ($\frac{7}{2}^+$ to $\frac{11}{2}^+$) and negative ($\frac{5}{2}^-$ to $\frac{11}{2}^-$) parity states in the intermediate energy region of the (^{3}He, α) spectra. A comparison up to 2.5 MeV is presented in Fig. 6.

The general trend of the experimental results (levels, excitation energies, spins, and parities) is rather well reproduced by the present unified model calculation, with, however, some discrepancies between theoretical and experimental spectroscopic factors. One notices that two-step pickup amplitudes may interfere with direct pickup ones and may thus modify the deduced C^2S for the levels above ~1 MeV which have obviously strong collective components.

C. Coupled-channels calculations for ^{115}Sn

Coherent coupled-channels calculations for the ^{116}Sn(^{3}He, α) ^{115}Sn reaction at 39 MeV were performed with the weak-coupling wave functions discussed in the preceding paragraph, using the code CHUCK.[18] The general features of these calculations, for purely collective states (pure two-step process only), are the following:

(i) Collective excitation in the α channel plays an important role and has to be taken into account, in addition to the ^{3}He channel.

(ii) The two inelastic form factors involved in the inelastic (^{3}He, ^{3}He′) or (α, α') channels were calculated using similar βR deformation lengths ($\beta_2 R = 0.72$ and $\beta_3 R = 0.82$).

(iii) The angular distribution of a level with total angular momentum J in a multiplet $|nlj \otimes 2^+\rangle_J$ is rather similar to that of a direct L, J equivalent pickup if $J = L + \frac{1}{2}\epsilon$, when $j = l + \frac{1}{2}\epsilon$ (with $\epsilon = \pm 1$). On the contrary, the members of the multiplet with $J = L - \frac{1}{2}\epsilon$ have a typical "bell" shape angular distribution and smaller cross sections.

In the excitation energy range $1.5 < E_x < 3.5$ MeV, most of the weak-coupling wave functions are a mixture of strong collective components plus a one hole component. These wave functions were used to perform coupled-channels calculations; a few typical comparisons between the resulting theoretical angular distributions and the experimental ones are presented in Fig. 7. Taking into account the complexity involved in such calculations, the agreement can be considered as acceptable. The new state observed at 1805 keV is well reproduced by the calculations assuming it is the $\frac{11}{2}^+$ member of the $|1g_{7/2} \otimes 2^+\rangle$ multiplet. As mentioned in (iii) above, we notice that the pure two-step curve is very similar to the $l = 6$ direct transfer one.

The one hole component generally dominates (due to matching conditions) the population of the other levels although the addition of the two-step amplitude changes significantly the predicted cross sections, partly solving the "apparent" discrepancy between predicted and observed C^2S. The spin assignments proposed for the strongest $L \geq 3$ "equivalent" direct transitions observed in the present experiment between ~1.0 and ~3.7 MeV are summarized in Table IV and Fig. 6.

We wish to draw attention to the observation of some weaker structures between ~2.9 and ~3.6 MeV having an $l = 5$ dominant behavior. They are in agreement with the weak-coupling picture which predicts several $\frac{11}{2}^-$ states in that region, due to the fragmentation of the $\frac{11}{2}^-$ member of the $|2d_{5/2} \otimes 3^-\rangle$ multiplet, by interaction with other multiplets (see Table IV). The wave functions of these states contain a significant $h_{11/2}$ quasihole component.

We would like to point out that these calculations also account for the shape and about half of the cross section of the 2600 keV peak, obviously complex in the (^{3}He, α) experiment while observed as

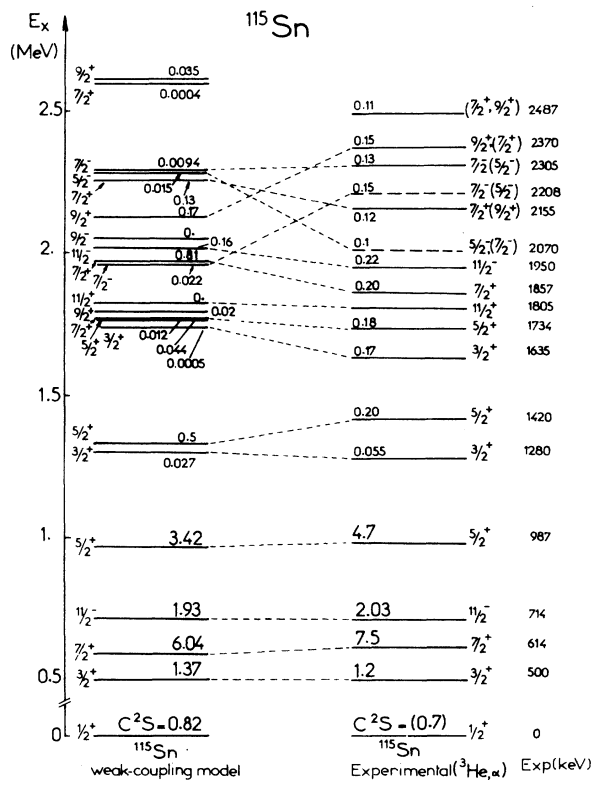

FIG. 6. Weak-coupling calculations for the ^{115}Sn nucleus. The experimental excitation energies, spins, parities, and spectroscopic factors are presented and compared to the corresponding theoretical predictions.

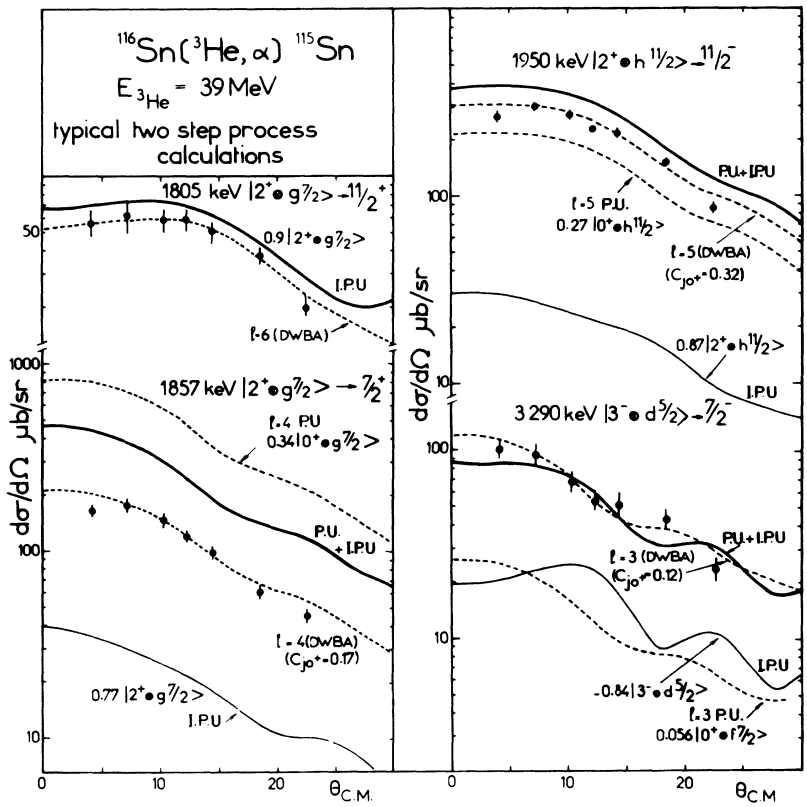

FIG. 7. Comparison between experimental angular distributions and two-step process calculations for some levels in ^{115}Sn. The weak-coupling model wave functions for such levels (with large collective components: see Table IV) were used in the calculation. Each state is labeled by its excitation energy, strongest collective wave function component $|I^\pi \otimes nlj>$, and proposed spin and parity J^π. The comparison with the data is made for pure direct pickup (DWBA or PU), pure indirect pickup (IPU), and combination of the two processes (PU+IPU).

a single peak and assigned pure $l=1$ in the (d,t) experiments.[2,3] The calculations describe this state as the $\frac{1}{2}^-$ member of the $|1g_{7/2} \otimes 3^-\rangle$ multiplet, with a quite large ($C_j 0^+ = 0.26$) inner hole component, in agreement with Koeling and Iachello's calculations[17] on the fragmentation of inner orbitals.

In summary, the (^{3}He, α) reaction has revealed or confirmed the observation of new states in the ~1.6 to ~3.7 MeV excitation energy region of ^{115}Sn; the population of such states is well reproduced by the weak-coupling model and two-step calculations.

The selectivity of the reaction allows the observation of rather high spin states with strong collective character, which are difficult to observe in (p,d) or (d,t) reactions or even in inelastic scattering, where only the population of states corresponding to the coupling of collective even core states with the $\frac{1}{2}^+$ ground state is strongly enhanced.

We have also shown the necessity of including the inner-hole states in the model, in order to explain some "anomalous" spin and parity states lying at low excitation energy. This fragmentation reveals a strong coupling between these inner-hole states, lying at rather high excitation energy (>5 MeV) and the first ($2^+, 3^-, \ldots$) collective states of ^{116}Sn.

D. The ^{112,120}Sn(^{3}He,α)^{111,119}Sn reactions

The neutron-hole distributions in ^{111}Sn and ^{119}Sn were investigated up to ~16 MeV excitation energy. The experimental data were recorded at two angles (4° and 12° laboratory angles) for comparison with the ^{115}Sn data. The neutron pickup data[4,16,19] on these nuclei are rather scarce and, for C^2S information, the only possible comparison with previous work was with the (p,d) study of Flemming,[4] which was, however, limited to the low-lying levels (up to 655 keV in ^{111}Sn and up to 2.2 MeV in ^{119}Sn). During the writing of the present paper, new (p,d) data[20] at 27.5 MeV incident energy on ^{112}Sn became available. No (^{3}He, α) experiment has previously been reported on these two nuclei.

Typical energy spectra are given in Fig. 2, obviously showing quite different features. This is not surprising in view of the weak-coupling picture

TABLE IV. ^{116}Sn(^{3}He, α)^{115}Sn: summary of J^π proposed assignments from weak-coupling calculation and two-step process analysis ($l \geq 3$).

E_x (experiment) (keV)	l [a] DWBA	Unperturbed multiplet E_x (keV)	$J^\pi_{(\text{proposed})}$	E_x (model) this work (keV)	Wave functions hole component + collective component
1805	6	$\lvert 2^+ \otimes g_{\frac{7}{2}}\rangle$	$\frac{11}{2}^+$	1824	$0 + 0.91\lvert 2^+ \otimes g_{\frac{7}{2}}\rangle + \cdots$
1857	4	~1900	$\frac{7}{2}^+$	1972	$-0.34\lvert 0^+ \otimes g_{\frac{7}{2}}\rangle + 0.77\lvert 2^+ \otimes g_{\frac{7}{2}}\rangle + \cdots$
1950	5	$\lvert 2^+ \otimes h_{\frac{11}{2}}\rangle$	$\frac{11}{2}^-$	2014	$0.27\lvert 0^+ \otimes h_{\frac{11}{2}}\rangle + 0.87\lvert 2^+ \otimes h_{\frac{11}{2}}\rangle + \cdots$
2208	(3)	~2000	$(\frac{7}{2}^-)$	1980	$-0.05\lvert 0^+ \otimes f_{\frac{7}{2}}\rangle + 0.94\lvert 2^+ \otimes h_{\frac{11}{2}}\rangle + \cdots$
2070	(3)	$\lvert 3^- \otimes s_{\frac{1}{2}}\rangle$	$(\frac{5}{2}^-)$	2280	$0.05\lvert 0^+ \otimes f_{\frac{5}{2}}\rangle + 0.99\lvert 3^- \otimes s_{\frac{1}{2}}\rangle + \cdots$
2305	3	~2270	$\frac{7}{2}^-$	2297	$-0.04\lvert 0^+ \otimes f_{\frac{7}{2}}\rangle + 0.98\lvert 3^- \otimes s_{\frac{1}{2}}\rangle + \cdots$
2155	4	$\lvert 2^+ \otimes d_{\frac{5}{2}}\rangle$	$\frac{7}{2}^+$	2257	$0.14\lvert 0^+ \otimes g_{\frac{7}{2}}\rangle + 0.86\lvert 2^+ \otimes d_{\frac{5}{2}}\rangle + \cdots$
2370	4	~2250	$\frac{9}{2}^+$	2125	$-0.13\lvert 0^+ \otimes g_{\frac{9}{2}}\rangle + 0.83\lvert 2^+ \otimes d_{\frac{5}{2}}\rangle + \cdots$
2807	(3)	$\lvert 3^- \otimes g_{\frac{7}{2}}\rangle$ ~2800	$(\frac{5}{2}^-)$	2852	$0.07\lvert 0^+ \otimes f_{\frac{5}{2}}\rangle + 0.89\lvert 3^- \otimes g_{\frac{7}{2}}\rangle + \cdots$
3070 [b]	(4) + 5	$\lvert 3^- \otimes h_{\frac{11}{2}}\rangle$ ~3000	$\frac{9}{2}^+$	2985	$0.063\lvert 0^+ \otimes g_{\frac{9}{2}}\rangle + 0.95\lvert 3^- \otimes h_{\frac{11}{2}}\rangle + \cdots$
		$\lvert 3^- \otimes d_{\frac{5}{2}}\rangle$ ~3250	$\frac{11}{2}^-$	~3300	$0.08\lvert 0^+ \otimes h_{\frac{11}{2}}\rangle - 0.52\lvert 3^- \otimes d_{\frac{5}{2}}\rangle + \cdots$
					or $0.05\lvert 0^+ \otimes h_{\frac{11}{2}}\rangle - 0.4\ \lvert 3^- \otimes d_{\frac{5}{2}}\rangle + \cdots$
					or $0.08\lvert 0^+ \otimes h_{\frac{11}{2}}\rangle - 0.37\lvert 3^- \otimes d_{\frac{5}{2}}\rangle + \cdots$
					or $\cdots$
3290	3		$\frac{7}{2}^-$	3271	$0.056\lvert 0^+ \otimes g_{\frac{7}{2}}\rangle - 0.84\lvert 3^- \otimes d_{\frac{5}{2}}\rangle + \cdots$

[a] Strongest $l \geq 3$ transitions observed in the (^{3}He, α) reaction.
[b] Doublet.

described above for ^{115}Sn. The quasihole valence energies involved vary quite strongly from one isotope to the other (as can be seen from the relative position of the first strongly excited $\frac{7}{2}^+$ and $\frac{5}{2}^+$ states as compared to the $\frac{11}{2}^-$ one). In addition, the evolution, although smoother, of 2^+ and 3^- phonon energies of doubly even Sn isotopes have to be taken into account.

From ~2.0 to ~3.6 MeV, the spectrum of ^{119}Sn appears obviously more complex than the one of ^{111}Sn. A comparison between C^2S values for the first strongly excited low-lying states of ^{111,115,119}Sn is presented in Table V, together with the results from previous (p,d) studies[4,20] and with the results of our weak-coupling calculations, extended to ^{111}Sn and ^{119}Sn. The results are now discussed for each isotope, in the framework of this model.

^{111}Sn. Above ~1.0 MeV excitation energy, very little is known about this isotope. In the present experiment, from ~1.0 to ~3.5 MeV excitation energy, the spectrum is dominated by previously unobserved strong structures located at 1280, 1470, 2070, and 2320 keV. The peak at 1280 keV is obviously complex and, although it includes the $\frac{5}{2}^+$ state observed at 1320 keV by Cavanagh,[19] its important population in the (^{3}He, α) experiment strongly suggests that a new level is populated by an $l > 2$ transfer. The first low-lying multiplet $\lvert 1g_{7/2} \otimes 2^+\rangle$ should lie around 1.26 MeV in ^{111}Sn (the 2^+ state in ^{112}Sn being at 1.26 MeV), with strong enhancement in the (^{3}He, α) reaction of the $\frac{7}{2}^+$ member of this multiplet; we therefore suggest that the new state at 1280 keV could possibly be the $\frac{7}{2}^+$ member of this multiplet. The second multiplet $\lvert 2d_{5/2} \otimes 2^+\rangle$ is expected around 1.41 MeV, with preferential enhancement of the $\frac{9}{2}^+$ member, as was observed in the ^{115}Sn case. We therefore tentatively assign $J^\pi = \frac{9}{2}^+$ to the 1470 keV state. Our proposed $J^\pi = \frac{7}{2}^+$ and $\frac{9}{2}^+$ for the levels at 1280 and 1470 keV are compatible with values of $(\frac{5}{2}, \frac{7}{2}, \frac{9}{2})^+$ proposed by Madueme in his γ-decay work[12] and in agreement with two-step DWBA calculations of the recent (p,d) work.[20]

Negative parity levels, based on the coupling between the 3^- state in ^{112}Sn (at $E_x = 2.35$ MeV) and the

TABLE V. Spectroscopic factors of the first low-lying levels in ^{111,115,119}Sn isotopes.

^{111}Sn						^{115}Sn					^{119}Sn				
E_x (keV)	l, J^π	C^2S [a]	C^2S [b]	C^2S [c]	C^2S [a] (model)	E_x (keV)	l, J^π	C^2S [a]	C^2S [b]	C^2S [a] (model)	E_x (keV)	l, J^π	C^2S [a]	C^2S [b]	C^2S [a] (model)
0	$4, \frac{7}{2}^+$	6	5	4.5	5.3	0	$0, \frac{1}{2}^+$	···	1.0	0.82	0	$(0, \frac{1}{2}^+)$	···	1.8	1.3
154	$2, \frac{5}{2}^+$	4.2	5.6	4.0	3.82	500	$2, \frac{3}{2}^+$	1.2	1.3	1.37	24	$2, \frac{3}{2}^+$	1.8	2.4	2.0
(254)	$(0, \frac{1}{2}^+)$	···	0.48	0.29	0.20	614	$4, \frac{7}{2}^+$	7.5	6.0	6.04	89	$5, \frac{11}{2}^-$	3.5	4.6	5.0
644	$2, \frac{3}{2}^+$	0.65	0.72	0.54	0.24	714	$5, \frac{11}{2}^-$	2.0	3.6	1.93	788	$4, \frac{7}{2}^+$	6.0	5.3	4.0
(755)	$(2, \frac{5}{2}^+)$	···	···		···	987	$2, \frac{5}{2}^+$	4.7	6.0	3.42	920	$(2, \frac{5}{2}^+)$	(0.16)	0.5	0.06
879	$5, \frac{11}{2}^-$	0.85	···	0.82	1.14						1090	$2, \frac{5}{2}^+$	2.6	4.0	2.5
											1355 (1385)	$2, \frac{5}{2}^+$	1.32	1.5	1.24
$\sum C^2S$		12.2 [d]	11.8	10.15	10.7			16.4 [d]	17.9	13.6			17.3 [d]	20.1	16.1
Maximum sum rule:				12					16					20	

[a] Present work.
[b] Reference 4.
[c] Reference 20.
[d] The $\frac{1}{2}^+$ state being mismatched in our experiment, we have added the more reliable C^2S $(\frac{1}{2}^+)$ value of Flemming (Ref. 4) to our other experimental C^2S.

$1g_{7/2}$ and $2d_{5/2}$ hole configurations are expected around ~2.4 MeV in ^{111}Sn. In addition, the $|1h_{11/2} \otimes 2^+\rangle$ multiplet is also expected in the same energy region, i.e., ~2.24 MeV. Thus, negative parity states should dominate above ~2 MeV in the ^{111}Sn spectrum and the strong and complex structures observed at 2070 and 2320 keV probably include, as in ^{115}Sn, levels corresponding to $l=5$ $(\frac{11}{2}^-)$ and $l=3$ $(\frac{5}{2}^-, \frac{7}{2}^-)$ transitions. This assumption is in good agreement with the proposal by Madueme[12] of a level at 2060 keV with $J \geq \frac{7}{2}$, negative parity.

^{119}Sn. In this isotope the $1g_{7/2}$ and $2d_{5/2}$ orbitals are usually assumed to be quite full. The corresponding $\frac{7}{2}^+_1$ and $\frac{5}{2}^+_1$ states lie above 750 keV, in a region where weak-coupling states are known to appear. (The one phonon 2^+ state lies at 1.17 MeV in ^{120}Sn and the two members of the $|3s_{1/2} \otimes 2^+\rangle$ multiplet have been observed around 920 keV.) A fragmentation of these orbitals is therefore expected while in ^{111}Sn the $\frac{7}{2}^+_1$ and $\frac{5}{2}^+_1$ are the two first excited states with rather pure hole character. The fragmentation of the $2d_{5/2}$ orbital is well established, the strength being appreciably split between at least two known[4,16,19] $J^\pi = \frac{5}{2}^+$ levels at 1090 and 1355 keV, while in ^{115}Sn the $\frac{5}{2}^+_1$ level still concentrates most of the strength. In the case of the $1g_{7/2}$ orbital and of the $\frac{7}{2}^+_1$ level (at 788 keV in ^{119}Sn), we emphasize the drastic decrease of the strength of this component as A increases, observed in our work between ^{115}Sn and ^{119}Sn and in the work of Flemming[4] between ^{115}Sn and ^{123}Sn. The $\frac{5}{2}^+_1$ and $\frac{7}{2}^+_1$ trends are reproduced by the weak-coupling calculations.

We wish to point out that the peak observed at 1355 keV in our experiment is obviously a doublet showing evidence, besides the known 1355 keV $(\frac{5}{2}^+)$ level, for a new state at ~1385 keV. The rather strong population of this state in the (^{3}He, α) reaction indicates the presence of a transition with $l>2$. It could possibly be the $l=4$ transition corresponding to the population of the $\frac{7}{2}^+$ member of the $|2d_{3/2} \otimes 2^+\rangle$ multiplet; this $\frac{7}{2}^+$ level has been observed from ^{123}Sn to ^{129}Sn in radioactivity work by Fogelberg *et al.*[21] and it has a much stronger calculated one hole component in ^{119}Sn ($C_f 0^+ = 0.41$) than in ^{111}Sn and ^{115}Sn, where it is almost purely collective ($C_f 0^+ \sim 0.04$).

It is clear that higher resolution data and complete angular distributions are needed for ^{111}Sn and ^{119}Sn (and other Sn isotopes) in order to further test the weak-coupling model in the intermediate excitation energy range, seldom investigated up to now.

V. INNER-HOLE STATES IN ^{111,115,119}Sn AND FRAGMENTATION OF THE $1g_{9/2}$ STRENGTH

As discussed above, very little hole strength is expected beyond 3.5 MeV excitation energy for the valence hole orbitals $(d_{5/2}, d_{3/2}, g_{7/2}, h_{11/2})$. Therefore the strong structures observed around 4.2, 5.4, and 5.6 MeV in the residual spectra of ^{111}Sn, ^{115}Sn, and ^{119}Sn (see Fig. 3) have been previously[1,3,5,6] attributed to neutron pickup from the

next inner orbital, i.e., the $1g_{9/2}$ orbital.

These structures (referred to in the following as "bump B") are clearly fragmented in rather well separated peaks or groups in ^{111}Sn and ^{115}Sn and to a lesser extent in ^{119}Sn. The fine structure first reported[1] for the $1g_{9/2}$ hole orbital in ^{115}Sn is clearly confirmed and even enhanced in this (^{3}He,α) experiment, as shown in Fig. 8. A detailed comparison of the fine structure, in the three Sn isotopes studied in the present work, is presented in Fig. 9. On both sides of the main structure (B), at smaller (region A) and higher (region C) excitation energies, weaker groups are also observed. Above 5.5, 6.5, and 7.0 MeV excitation energies, the ^{111,115,119}Sn spectra no longer present noticeable fine structure, but rather broad and weak structures (around 9 MeV in ^{115,119}Sn) and slowly decreasing cross section (see Fig. 3). A flat continuous background is finally observed in the en-

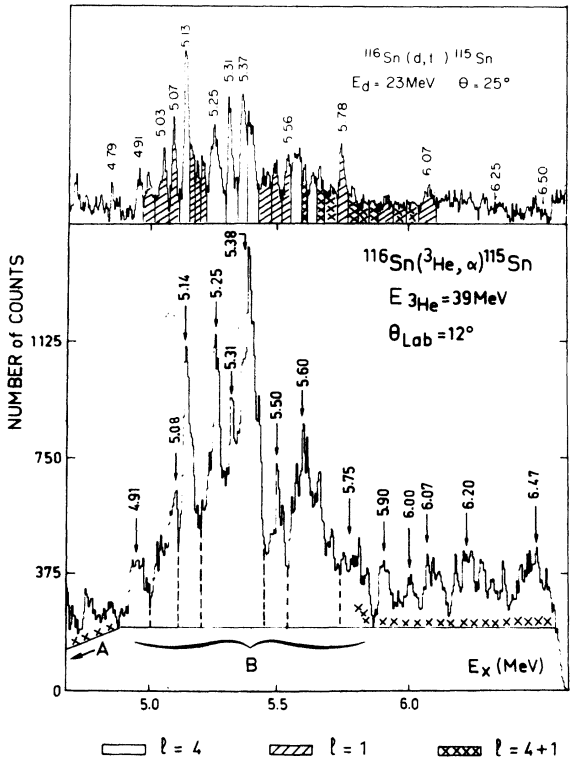

FIG. 8. Detailed comparison between the "fine structure" of the $1g_{9/2}$ inner hole state in ^{115}Sn as observed in the (d,t) and (^{3}He, α) reactions. One can clearly notice the enhancement of the $l=4$ levels in the (^{3}He, α) spectrum, as compared to the (d,t) spectrum. The numbers on top of the peaks or groups refer to the centroid energies or dominant structure position of the adjacent slices used in order to extract the angular distributions of these fragmented and narrow structures. They were consistent with the ones chosen in the (d,t) study. The limits of each slice are indicated.

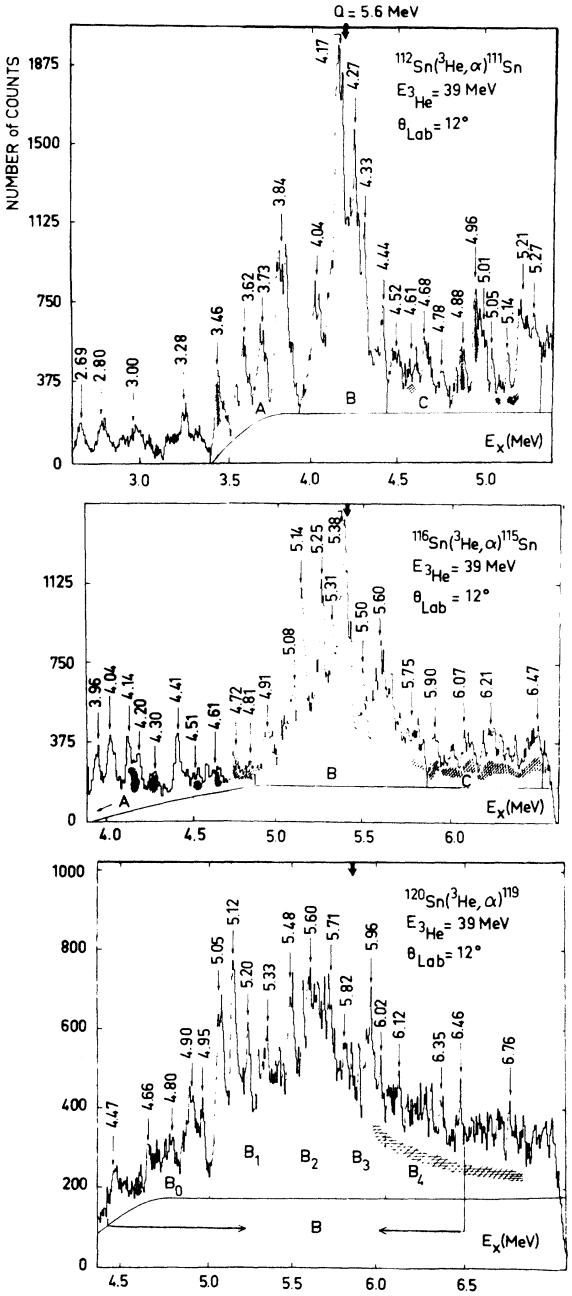

FIG. 9. Comparison of the fragmentation and spreading of the $1g_{9/2}$ inner-hole orbital in the ^{111,115,119}Sn isotopes (fine structure regions A, B, and C). Peaks or groups of peaks are labeled by the centroid energy of the adjacent slices used in the analysis in order to extract the angular distributions and C^2S of these fragmented structures (see Table VI). Typical deduced angular distributions for ^{115}Sn are also presented in Fig. 10. The vertical and horizontal solid lines indicate, respectively, the limits of the "bump" regions (A, B, C, see text Sec. V) and the background level used in the analysis of the date. One can clearly notice the broadening of the main structure B when the mass number increases (A = 111 to 119). Shaded areas correspond to a mixing of $l=4+1$ transitions.

ergy range of the analog states ($E_x \gtrsim 10$ MeV).

In order to carry out a detailed analysis of the structures observed in the three isotopes, the "fine structure" part of the residual spectra was divided into adjacent slices chosen after a careful comparison of the behavior of the spectra at all angles. The main part of the bump B has limits which are consistent with the ones chosen by Van der Werf *et al.*[3] in their study of the (d, t) reaction on the tin isotopes and correspond to the narrow $l=4$ part of the observed structures. All the deduced cross sections were determined after subtraction of a continuous background (as defined in Figs. 3 and 9) which smoothly connects the flat part at high excitation energies to the minima of the cross section observed at all angles in the lower energy range (i.e., 3–3.5 MeV). In the absence of any prediction for the background shape and magnitude, the adopted procedure seems to be the most consistent one in order to extract the peaks or structures cross sections. One can notice in Fig. 9 that the region A, corresponding to strong discrete peaks in ^{111}Sn and to some weaker states in the two other isotopes, is observed above a rising background. The upper, decreasing part of the bump (region C) does not contain narrow states or groups in ^{119}Sn and was not considered in the analysis of this isotope.

A. *l* identification

Typical angular distributions of different slices of the ^{115}Sn spectrum are presented in Fig. 10 together with the corresponding DWBA curves. The ratio R of the cross sections at 4° and 12° laboratory angles are given for the three Sn isotopes in Table VI.

In ^{115} Sn, the main features of these results are the following.

The angular distributions of the peaks in region B are all very similar and are individually best fitted by the $l=4$ DWBA prediction. The whole region B is nicely reproduced by an $l=4$ transfer as shown in Fig. 10. The strongest peaks previously observed in the (d, t) experiment also corresponded to an $l=4$ transfer, but some groups in the same excitation energy range were also populated through an $l=1$ transfer. It is clear from Fig. 8 that the angular momentum matching in the (^{3}He, α) reaction, near 5 MeV excitation energy in ^{115}Sn, strongly enhances the $l=4$ as compared to the $l=1$ transition. This leads to a more reliable determination of the $l=4$ strength in the main structure, as compared to previous (d, t) or (p, d) studies.

Region A exhibits also rather pure $l=4$ states, while around 4.5 MeV, contributions of levels with $l=1$ transfer are observed. Additional $l=4$ strength is observed in region C, but almost all the levels or groups of levels have their angular distributions obviously modified by $l=1$ contributions (see Table VI). Such $l=1$ strength around 4.2 and 6.2 MeV in ^{115}Sn is in overall agreement with previous works.[3]

In the excitation energy range above region C,

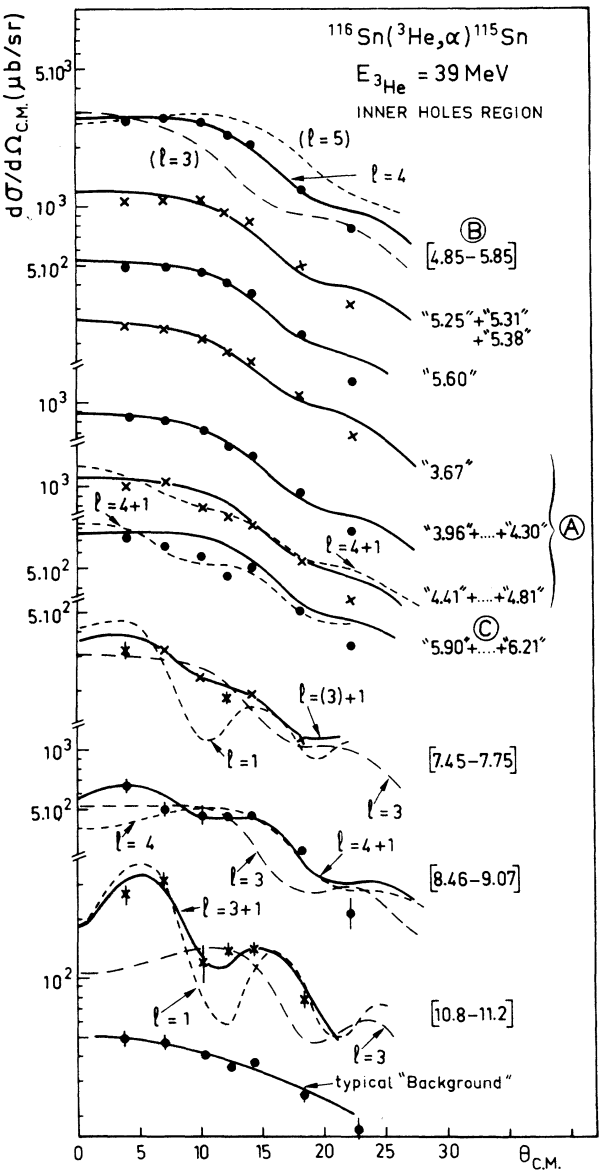

FIG. 10. Typical angular distributions of peaks or groups of peaks belonging to the "inner neutron-hole region" in ^{115}Sn. The angular distribution for each slice or group of slices, labeled by its energy limits or centroid, is compared to one-step DWBA calculations assuming $l=4$, $l=4+1$, or $l=3+1$ angular momentum transfers. In the high excitation energy range ($E_x > 6.2$ MeV) indications of $l=1$, $2p$, components are clearly observed. A typical background angular distribution ($5 < E < 13.5$ MeV) is also presented for comparison.

the angular distributions of slices around 7.5, 8.5, and 11 MeV are reported in Fig. 10. The rising shapes at forward angles demonstrate the population of $l=1$ components. This evidence is especially clear at 11 MeV. At this excitation energy, the matching condition for an $l=1$ transfer becomes reasonably fulfilled. We would like to point out the large spreading of the $l=1$ components (4 MeV$< E_x <$11 MeV) in ^{115}Sn.

Turning now to the ^{111}Sn and ^{119}Sn results, one can notice the rather small and constant ratio R in the whole region B (see Table VI). These results, compared to those obtained for ^{115}Sn, suggest the population of $l=4$ components, in agreement with previous works.[3,5,6] In ^{111}Sn, the new group of levels observed in region A seems also to have pure $l=4$ character and carries an appreciable amount of the $1g_{9/2}$ hole strength. The region C exhibits a number of narrow states in ^{111}Sn, whereas in ^{119}Sn almost no fine structure is observed in the tail of the main structure B.

B. Fragmentation and observed strength of the $1g_{9/2}$ inner hole

The spectroscopic factors for each individual peak or group of peaks observed in the "fine structure" energy range (regions A, B, and C) for ^{111}Sn, ^{115}Sn, and ^{119}Sn are reported in Table VI. The mean excitation energy, width, and total spectroscopic strength of the main structures are summarized in Table VII. We would like to emphasize the following points.

TABLE VI. Detailed analysis of the fine structure region in the ^{112,116,120}Sn(^{3}He, α)^{111,115,119}Sn reactions.

	^{111}Sn					^{115}Sn					^{119}Sn			
	"E_x" [a] (MeV)	R [b]	l	C^2S ($1g_{9/2}$)		"E_x" [a] (MeV)	R [b]	l	C^2S ($1g_{9/2}$)		"E_x" [a] (MeV)	R [b]	l	C^2S ($1g_{9/2}$)
A	3.46	2.3	(4)+1	(~0.05)	A	3.67	1.35	4	0.20	A	3.89	1.25	4	0.07
	3.62	1.1	4	0.20		3.96	1.3	4	0.15		3.98	1.30	4	0.08
	3.73	1.15	4	0.33		4.04	1.37	4	0.17		4.05	1.35	4	0.06
	3.82, 3.86	1.0	4	0.63		4.14, 4.20	1.44	4(+1)	0.23		4.21	1.40	4	0.11
				$\sum$=1.21		4.3	1.46	4(+1)	0.11					$\sum$=0.32
B	4.04	1.15	4	0.48		4.4	1.35	4	0.15	B_0	4.47	1.4	4	0.03
	4.17	1.20	4	0.97		4.51	1.45	4(+1)	0.06		4.66, 4.80	1.35	4	0.10
	4.27	1.1	4	0.58		4.61	1.7	4+1	0.09		4.90, 4.95	1.45	4	0.14
	4.33	0.9		0.21		4.72, 4.81	1.6	4+1	0.104					
	4.44	0.95	4	0.40					$\sum$=1.30		5.05	1.5	4	0.18
				$\sum$=2.6						B_1	5.12	1.4	4	0.15
C	4.52	1.05		0.30		4.91	1.38	4	0.12		5.20	1.4	4	0.10
	4.61	1.3	4(+1)	0.35		5.08	1.34	4	0.20		5.33	1.55	4	0.33
	4.68	1.15	4	0.35		5.14	1.16	4	0.30					
	4.78	0.75	4	0.25		5.25, 5.31, 5.38	1.11	4	1.07	B_2	5.48	1.5	4	0.18
	4.88	1.89	1		B	5.50	1.23	4	0.13		5.6, 5.71	1.5	4	0.55
	4.96, 5.01	1.30	4(+1)	0.15		5.60	1.20	4	0.47					
		1.05	4	0.2		5.75	1.50	4(+1)	0.27	B_3	5.82	1.5	4	0.2
	5.05	1.09	4	0.15					$\sum$=2.56		5.96, 6.02	1.6	4(+1)	0.27
	5.14			(0.15)										
	5.21, 5.27		(4), (4)	(0.50)		5.90, 6.0, 6.07	1.60	4+1	0.35	B_4	6.12, 6.30, 6.36	1.75	4+1	~0.3
				$\sum$=2.40							6.46	1.90		
	Percentage of the total $1g_{9/2}$ strength			62%	C	6.21	1.65	4+1	0.28					$\sum$=2.5
						6.47		4+1	0.21		Percentage of the total $1g_{9/2}$ strength			≲28%
									$\sum$=0.84					
						Percentage of the total $1g_{9/2}$ strength			43% [c]					

[a] "E_x" refers to the energy centroid (or energy of the dominant structure) of each of the adjacent slices. It corresponds to the energy given in Figs. 8 and 9.

[b] $R=\sigma(4°)/\sigma(12°)$.

[c] An estimate of the $l=1$ contribution has been subtracted from the partial sums given above. These partial sums were obtained assuming pure $l=4$ transfer.

TABLE VII. Summary of measured strengths and widths for the main part of the fine structure region.

		This work				(d,t) [b]				C^2S (other works)			
	E_x (MeV)	$\bar{E}_x$ (MeV)	σ [a] (keV)	FWHM [a] (keV)	C^2S	$\bar{E}_x$ (MeV)	σ [a] (keV)	FWHM [a] (keV)	C^2S	(d,t)	(p,d)	$(^3\mathrm{He},\alpha)$	C^2S Theo [g]
^{111}Sn	(3.4–4.5) A+B	4.07	245	575	3.8	3.95	300	705	2.5		3.3 [d]		6.7
	(4– 4.5) B	4.22	130	300	2.6						2.02 [d]		6.7
^{115}Sn	(4.8–5.8) B	5.47	246	580	2.5	5.20	240	560	2.5	1.5 [c]	1.9 [e]	1–2 [e] 1.3 [f]	7.8
^{119}Sn	(4.3–6.5) B	5.61	446	1050	2.5	5.45	470	1100	2.5			2.2 [f]	8.0–9.7

[a] $\sigma=(\sum_i C^2S_i(E_i-\bar{E})^2/\sum_i C^2S_i)^{1/2}$, FWHM $=2.35\sigma$.
[b] Reference 3.
[c] Reference 1.
[d] Reference 20.
[e] Reference 5.
[f] Reference 6.
[g] Reference 17.

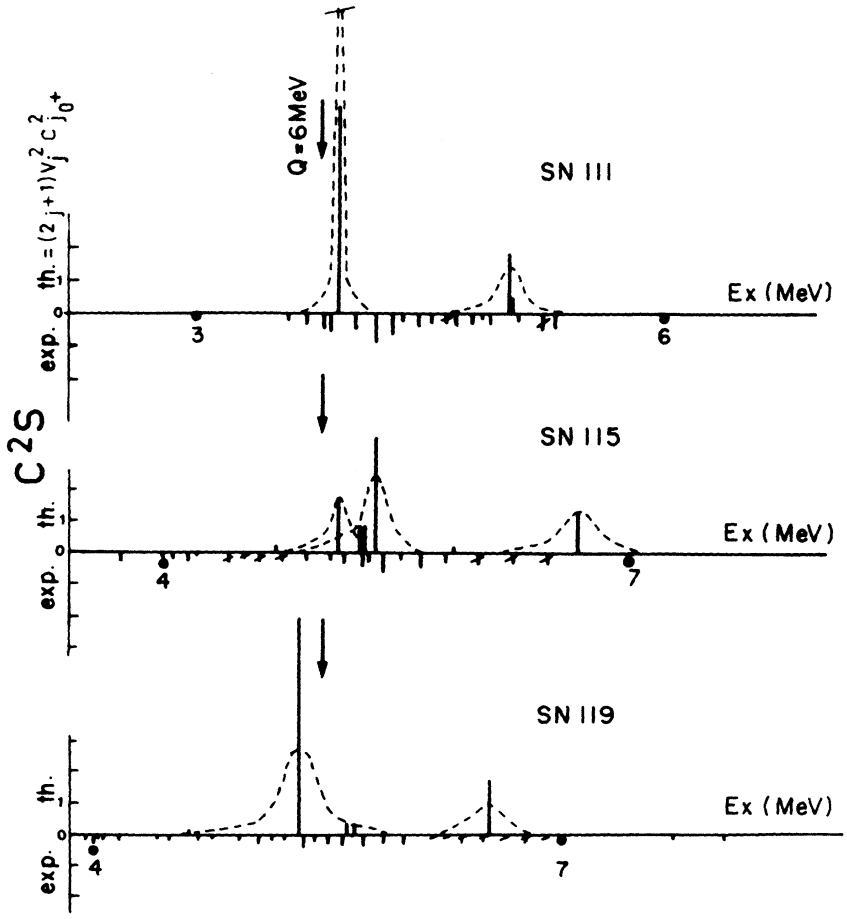

FIG. 11. Comparison of the experimental fragmentation of the $1g_{9/2}$ inner-hole orbital with the calculations of Koeling and Iachello (Ref. 17) for the ^{111}Sn, ^{115}Sn, and ^{119}Sn isotopes. The size of vertical bars represents the strengths of the $1g_{9/2}$ in the displayed energy range for both the experimental states and the theoretically predicted ones. The dashed curves represent the calculated spreading of the $1g_{9/2}$ inner-hole orbital in the Sn isotopes. The vertical bars crossed by an oblique line indicate the regions where $l=1+4$ or $l=1+3$ strength has been observed (not pure $l=4$ regions). The calculation predicts a splitting of the $1g_{9/2}$ neutron-hole strength into two main structures. The weaker one, predicted around 5.1, 6.6, and 6.5 MeV in the ^{111,115,119}Sn isotopes, comes from the coupling of the $1g_{9/2}$ hole with the 2_1^+ level of the even-even target nuclei.

The most striking result is the observation in the three isotopes of a limited number of narrow peaks which have an $l=4$ angular distribution. It is also interesting to notice the evolution of the fine structure with the mass number, leading to very small peaks superimposed on a wider bump in ^{119}Sn (see Fig. 9).

The narrowest part of the bump (region B), as deduced from this analysis, accounts for about 25% of the $1g_{9/2}$ sum rule limit in the three isotopes. This result, and also the deduced widths, agree with those of Ref. 3 for ^{115,119}Sn. In the case of ^{111}Sn, some discrepancies are observed between the present results and those of Ref. 3. In that study of the (d, t) reaction region A was not separated from the main structure, but the total strength observed in regions A+B was only 25% as compared to the 38% measured in the (^{3}He, α) reaction in the same energy interval; the deduced widths in the two experiments are not consistent (see Table VII). We do not observe the minimum in the width of the main bump for ^{115}Sn. This minimum, attributed to subshell closure, is certainly not very pronounced and remains a puzzling problem.

The total strengths, measured for the whole A+B+C region, decrease from 62% to 43% and 28% from ^{111}Sn to ^{115}Sn and ^{119}Sn. These figures might be increased by choosing a different background but will, in any case, remain rather low as compared to the sum rule limit. Part of the missing strength seems, according to the present experiment (see Fig. 10), somewhat spread up to rather high excitation energy (~10 MeV), in agreement with (^{3}He, α) experiments[6,7] at high energy ($E \gtrsim 100$ MeV) on Sn isotopes. These last experiments give rather large $l=4$ or 3 contributions up to 8–11 MeV excitation energy. Further experiments are needed to settle this point.

It is worthwhile to recall that standard DWBA analysis may not be well suited for highly fragmented hole states. The use of a standard form factor may be questionable but, in addition, other effects may also play a role. For example, if large collective components exist in the wave functions, preliminary estimates of two-step effects indicate small corrections of the main structure strength, but rather large effects (50% to 100%) in the high energy tail of the strength distribution.

C. Discussion

The observed fragmentation in the three isotopes are compared in Fig. 11 with the predictions of Koeling and Iachello.[17] According to these authors the $1g_{9/2}$ inner-hole strength is first fragmented over the collective three and five quasi-particle (qp) states (1 phonon—1 qp and 2 phonons—1 qp states). An additional spreading results from the small mixing of these collective states with the many close-lying noncollective three and five qp states; the combined fragmentation and spreading widths are predicted to increase from ^{111}Sn to ^{119}Sn, in agreement with the present experimental trend for the main structure B (see Table VII). The theoretical strengths are, however, much larger than the experimental ones and the strong fragmentation observed is not at all reproduced.

A very recent report by Vdovin *et al.*[22] gives somewhat different predictions for the $1g_{9/2}$ strength. In a 1 MeV energy interval around the main structure, in ^{111,115,119,121}Sn, these authors obtain 49% to 43% of the strength and typically 45% for ^{115}Sn as compared to 75% in Ref. 17 and to 25% experimentally observed. This strength decreases from $A=111$ to $A=119$ in agreement with experiment where, however, this effect is much more pronounced. The improved agreement with experiment is attributed to the following features: First, the calculation includes $\lambda > 3$ phonons in addition to the quadrupole (2^+) and octupole (3^-) vibrations, which nevertheless play a major role in the fragmentation. Second, the quasiparticle-phonon interaction strengths and the level density are somewhat larger. This increases both the strengths of the 1 phonon qp fragments (the doorway states) and the spreading by coupling with complicated states. Anyway, none of the two calculations[17,22] is able to reproduce the strong fragmentation revealed in the observed fine structure.

In Ref. 22, the spreading is described by a phenomenological spreading width Δ (500 keV) which seems too large, taking into account the experimental results, at least for ^{111}Sn, as shown in Table VII. In this nucleus (and partly in ^{115}Sn), the fragmentation into two or three main groups of strong peaks is the main feature. According to Nomura,[23] such groups of peaks, as observed in ^{111,115}Sn(^{119}Sn) on the low energy side of the main $1g_{9/2}$ structure, may be related to coupling effects with proton core polarized states. Anyway, in spite of the uncertainties in the experimentally deduced absolute spectroscopic factors, it seems that a significant part of the strength may lie at higher excitation energies, up to 9–11 MeV. It would be interesting to consider, in particular, the coupling with the octupole resonance (LEOR) recently observed in even-even Sn isotopes near 6.2 MeV excitation energy[24] with a strength leading, for example, in ^{115}Sn to the same β value as the one observed for the 3_1^- state.

VI. NEUTRON PICKUP TO ANALOG STATES IN ^{111,115,119}Sn

The neutron pickup reaction is well known to excite[25] in the residual nuclei both $T_<$ and $T_>$ components of an isospin doublet. Until recently, the available data on hole analog states were limited to a large extent to $T_>$ states in medium weight nuclei. However, the advent of high energy beams associated with sufficient energy resolution in the exit channel have allowed the investigation of such narrow levels in heavy nuclei[3,5,7,10,26,27] and some very recent results have been obtained on hole-analog states[28-30] in ^{143}Sm and ^{207}Pb. In spite of a severe reduction of the hole strength, owing to the isospin factor $1/2T_>$, narrow states are still observable in transfer reactions at high excitation energies (10 to 20 MeV) above a continuous background.

These structures are of importance because they involve many aspects of nuclear structure and reactions (i.e., Coulomb displacement energy, total widths, and mixing of the "doorway" states with the surrounding $T_<$ levels, spectroscopic strengths and DWBA analysis of "deeply bound" states, etc.).

A simple calculation of Coulomb displacement energy shows that the ground-state analogs in ^{111,115,119}Sn should appear around 10.4, 13.3, and 15.0 MeV excitation energy, respectively. The observed α spectra in the excitation energy range of interest are presented in Fig. 12 for the three isotopes. In each residual nucleus one clearly observes a number of sharp levels standing above the continuum. These levels have both correct spacings and relative cross sections with respect to the excitation energies, angular momentum transfer, and spectroscopic factors of their parent states in the In isotopes.[31-33] The first three analog states in ^{115}Sn and ^{119}Sn had been previously reported[3,5] in (p,d) and (d,t) reactions on ^{116,120}Sn. Three new analog states in ^{115}Sn, two new in ^{119}Sn, and the first four, previously unknown, analog states in ^{111}Sn have been observed in the present work.

These levels are located well above the proton, neutron, and α thresholds (for example $S_p = 8.73$ MeV, $S_n = 7.53$ MeV, $S_\alpha = 3.20$ MeV in ^{115}Sn) and their total intrinsic widths Γ have been extracted from the measured peak shapes by unfolding the experimental resolution (identified with the one obtained for bound states). Owing to our finite resolution (38 keV) this procedure limits the accuracy of Γ to 10–15 keV. The excitation energies and total widths for all the analog states observed are reported in Table VIII.

Recently, Bechetti *et al.*[34] have measured the total width of analog states in Sb and I isotopes

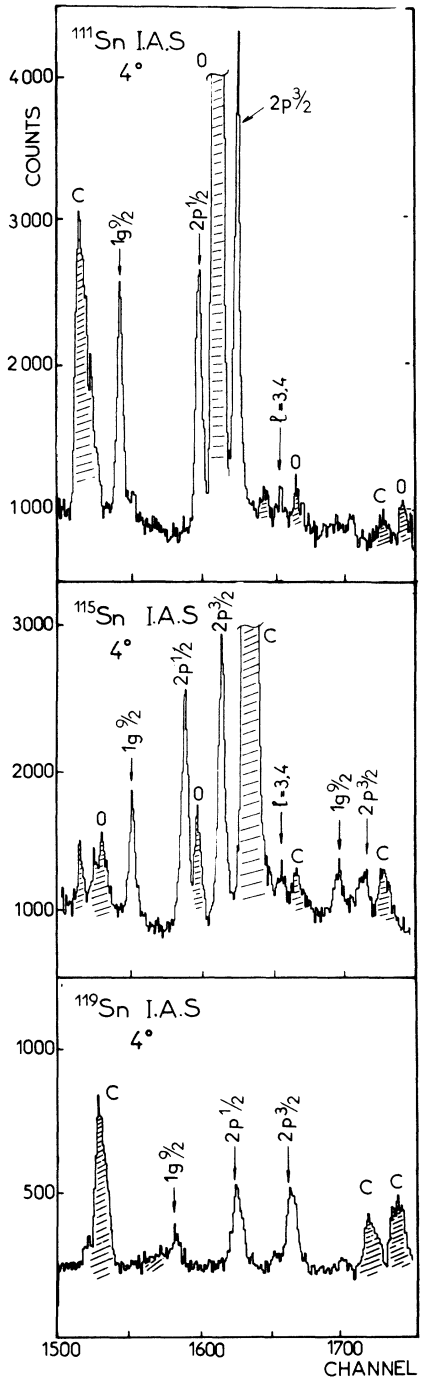

FIG. 12. The α energy spectra from the ^{112,116,120}Sn $(^3\mathrm{He},\alpha)^{111,115,119}$Sn reactions in the energy range where the $T_>$ components of the $1g$ and $2p$ inner-hole states are expected. One can notice, besides the strong peaks from ^{12}C and ^{16}O contaminants, a number of strongly excited narrow states. These levels, labeled by their neutron-hole configuration, are the analog states of the $1g_{9/2}$, $2p_{3/2}$, and $2p_{1/2}$ low-lying levels in the In isotopes.

TABLE VIII. Summary of the results of the analysis of the (^{3}He, α) reaction to hole-analog states in Sn isotopes.

Final nucleus	E_x (IAS) (MeV)	Γ (keV)	$E_x - E_0$ [a] (MeV)	E_x (parent) [b] (MeV)	J^π (parent) [b]	l c	J^π c	$(2T_0+1)C^2S_n$ [d] (^{3}He, α) [c] SE	CC	(p,d) [e] SE	CC	(d,t) [f] SE	C^2S_p (d, ^{3}He) [b] SE	SE
^{115}Sn	13.260 ± 0.015	31 ± 10	0.0	0.0	$\frac{9}{2}^+$	4	$\frac{9}{2}^+$	12.1	8.6	7.7	6.2	7.1	5.7	6.7	7.4
	13.630 ± 0.015	44 ± 10	0.370	0.340	$\frac{1}{2}^-$	1	$\frac{1}{2}^-$	2.2	1.1	2.3	1.4	1.9	1.2	1.5	1.7
	13.890 ± 0.015	44 ± 10	0.630	0.600	$\frac{3}{2}^-$	1	$\frac{3}{2}^-$	2.7	1.4	2.6	1.5	2.4	1.7	1.9	2.0
$T_> = \frac{17}{2}$	14.33 ± 0.020	>40	1.070	0.93 1.04 1.08	$(\frac{5}{2})^-$	(3) $(\frac{5}{2}^-)$ or (4) $(\frac{9}{2})^+$		4.01 3.25	2.0 2.3						0.7
				1.45	$(\frac{1}{2}, \frac{3}{2})^-$									0.3	0.5
	14.76 ± 0.02	50 ± 15	1.900	1.47		4	$\frac{9}{2}^+$	5.41	3.8						
				1.48	$(\frac{9}{2})^+$									2.9	2.4
	14.93 ± 0.025	···	1.660	1.65	$(\frac{1}{2}, \frac{9}{2})^-$	1	$(\frac{3}{2})^-$	0.54	0.28					0.4	0.4
^{111}Sn	10.47 ± 0.015	25 ± 10	0.0	0.0	$\frac{9}{2}^+$	(4)	$(\frac{9}{2})^+$	9.8	7.9				5.5		
	11.06 ± 0.020	25 ± 10	0.59	0.54	$\frac{1}{2}^-$	(1)	$(\frac{1}{2})^-$	2.0	1.1				1.5		
$T_> = \frac{13}{2}$	11.34 ± 0.020	30 ± 10	0.87	0.81	$\frac{3}{2}^-$	(1)	$(\frac{3}{2})^-$	2.2	1.1				2.0		
	11.78 ± 0.020	35 ± 10	1.31			(4) or (3)	$(\frac{9}{2})^+$ $(\frac{5}{2})^-$	1.50 1.25	1.20 0.73						
^{119}Sn	14.98 ± 0.020	30 ± 10	0.0	0.0	$\frac{9}{2}^+$	(4)	$(\frac{9}{2})^+$	12.0	7.60	7.2	5.5		5.9		6.5
	15.34 ± 0.020	40 ± 15	0.36	0.315	$\frac{1}{2}^-$	(1)	$(\frac{1}{2})^-$	1.5	0.74	1.7	0.98		1.2		1.6
$T_> = \frac{21}{2}$	15.63 ± 0.020	50 ± 15	0.65	0.610	$\frac{3}{2}^-$	(1)	$(\frac{3}{2})^-$	1.35	0.70	2.0	1.2		2.1		1.4
	16.10 ± 0.030	70 ± 20	1.12	1.050	$(\frac{5}{2})^+$	(1)	$(\frac{3}{2})^-$	(1.15)	(0.60)						(0.5)
	16.47 ± 0.03		1.49	1.45	$\frac{9}{2}^+$	(4)	$(\frac{9}{2})^+$	(4)	(2.6)						2.90

[a] E_0 is the excitation energy of the ground-state analog from this work.
[b] Excitation energies, spins and parities, and spectroscopic strengths for the parent states in In isotopes are taken from Refs. 31, 32, and 33.
[c] Present work.
[d] The C^2S_n values deduced from the analysis of $T_>$ states in Sn isotopes were multiplied by $(2T_0+1)$, where T_0 is the isospin of the target ground state, in order to allow a direct comparison with the spectroscopic strength C^2S_p of their parent states.
[e] Reference 5.
[f] Reference 3.

by means of the (^{3}He, t) reaction. The values obtained by these authors, in a very close mass region of the periodic table, are in good agreement with the ones listed in Table VIII for the Sn isotopes. A very recent high resolution study of the (p,d) reaction on the Sn isotopes[35] leads to comparable results for the measured widths of the $1g_{9/2}$, $2p_{3/2}$, and $2p_{1/2}$ $T_>$ states.

In order to obtain spectroscopic information on the $T_>$ states in the Sn isotopes, angular distributions have been measured for the six analog states in ^{115}Sn from 4° to 22° laboratory angles. Only two angles (4° and 12°) have been recorded in the case of ^{111}Sn and ^{119}Sn. The experimental results were compared to DWBA predictions using the parameters listed in Table I and the normalization constant $N=23$. For the bound state wave function, the procedure was somewhat different from the one employed for the $T_<$ states. It has already been noticed that the separation energy method (SE) was questionable[36] for levels with large separation energies ($B_n \gtrsim 20$ MeV); the corresponding form factors have small amplitudes at the nuclear surface where the DWBA method is expected to be a good approximation. Therefore, in addition to the usual SE procedure, we have calculated the neutron form factors for the $T_>$ states by solving the Lane coupled-channels equations (CC) for an isobaric analog pair.[37] An isovector term $4U_1(r)\, t\cdot T/A$ for the coupling strength, with $U_1(r) = -V_1' df(x)/dx$ and $f(x) = [1+\exp(r - r_0 A^{1/3}/a)]^{-1}$ with $x = (r - r_0 A^{1/3}/a)$, was used in the calculations. The term V_1' (116 MeV) is related to the usual isospin coupling strength $V_1 = 25$ MeV (Ref. 38) by the expression $V_1 = 2aV_1'/r_0 A^{1/3}$. A modified version of the computer code DNUM [39] was employed to solve the CC equations.

The results of such calculations are compared to the experimental distributions in Fig. 13. One should notice that the shapes of the theoretical curves are not dependent on the method used to compute the neutron form factor. The spectroscopic strengths are presented in Table VIII for the $T_>$ states in the three isotopes, together with the spectroscopic information already known from previous studies[3,5,10,26] or for their parent levels.[31-33] They are compared, in case of ^{115}Sn, to the results of Sekiguchi *et al.*[5] and Van der Werf *et al.*[3] and to their parent states proton hole strengths [$C^2S_p = (2T_0+1)\, C^2S_n$, where T_0 is the isospin of the target nucleus] deduced from (d, ^{3}He) studies.[31-33]

The results of this analysis of the $T_>$ states in the Sn isotopes suggest the following comments:

(i) The shapes of the angular distributions (see Fig. 13) are rather well reproduced by the DWBA calculations. The $l=1$ transfers are the best fitted by the calculations; at these excitation energies the (^{3}He, α) reaction is well matched for the $l=1$ transition. The maxima (4° laboratory) and minima (12° laboratory) are very characteristic of an $l=1$ transfer. This result has been used to estab-

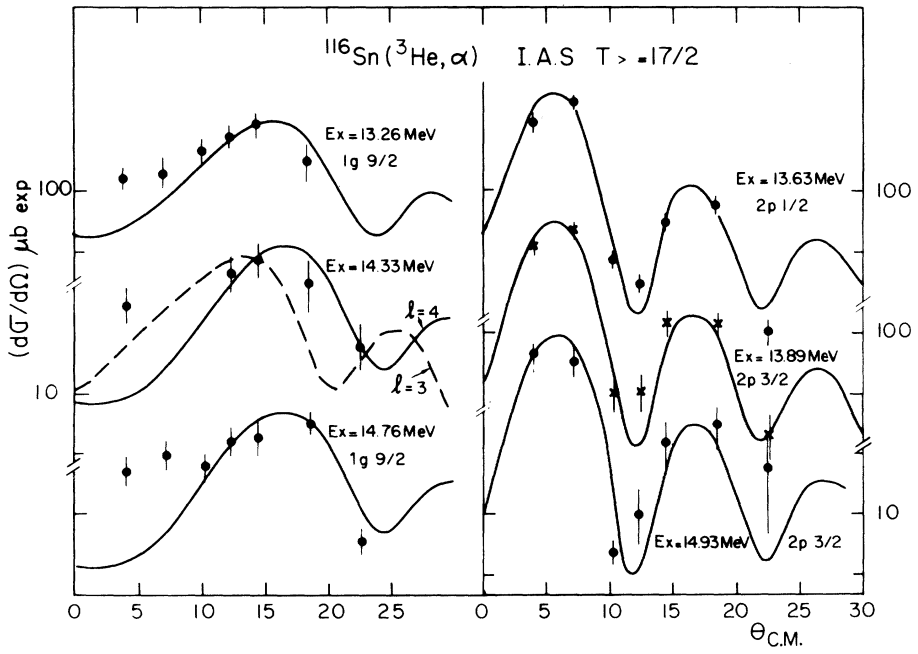

FIG. 13. Angular distributions of isobaric analog states in ^{115}Sn.

lish rather unambiguously the $l=1$ character of several analog states in ^{111,119}Sn (see Table VIII), for which only these two points have been measured.

The $l=4$ angular distributions are also in overall agreement with the data. Only the very forward angle data (4°–7°) are systematically higher than the theoretical predictions (see Fig. 13). This could reflect the angular momentum mismatch ($\Delta l \sim 3$) expected for such high l transfer. The ratio of the experimental cross sections at 4° and 12° laboratory angles is very close to 1 and also very characteristic of an $l=4$ transfer. This ratio was used in order to assign an $l=4$ transfer to the $E_x = 10.47$ MeV level in ^{111}Sn and to the $E_x = 14.98$ and 16.47 MeV levels in ^{119}Sn (see Table VIII).

(ii) As expected from previous analysis on hole-analog states,[3,5,10,27,29,30,33,40] the separation energy procedure leads to spectroscopic factors on the average much higher than the corresponding ones for parent levels (see Table VIII). The disagreement is larger for the $l=4$ transitions than for the $l=1$ transitions. Additional effect due to angular momentum mismatch, as reflected already by the shape of the angular distributions, could be a possible explanation to these observations. The main argument which demonstrates the failure of the SE method comes from the fact that the deduced C^2S_n strength is larger than or equal to the sum rule limit for the already fragmented $g_{9/2}$ and $p_{1/2}$ components.

These discrepancies are reduced by the use of the CC approach (see Table VIII). However, as mentioned in previous DWBA analysis of hole-analog states in heavy nuclei,[10,26,29,30] a consistent comparison with the parent states spectroscopic strengths can only be made if one uses the proton form factor from the Lane coupled equations to deduce the C^2S_p values. These calculations were performed for the low-lying states in ^{115}In and lead to C^2S_p values lower by about 40–50% than the ones listed in the corresponding column in Table VIII. Under such conditions, the observed discrepancies between $(2T_0+1)$ C^2S_n and C^2S_p remain large (50–60%) for the $l=4$ transitions and within the uncertainties of the DWBA calculations (15–25%) for $l=1$ transitions. Moreover, the introduction of the same isospin dependent part in the nuclear potential for the analysis of the $T_<$ states would increase the deduced C^2S_n strengths by about 30–40%, depending on the energy of the final states.

(iii) A more definite indication of the limits of the CC approach in the analysis of the $T_>$ states in heavy nuclei comes from the energy splitting

$$\Delta E_T = 4(T_0 + \tfrac{1}{2})\langle lj|U_1(r)|lj\rangle/A\,,$$

between the $T_<$ and $T_>$ components of a single hole state. Using as before the surface peaked interaction, $U_1(r)$ corresponding to $V_1' = 116$ MeV, leads to values lower than the experimental ones by about 4 MeV ($\Delta E_T \sim 7.8$ MeV for ^{115}Sn). Similar behavior have been already observed in the case of the splitting of the hole states[10,26,29,30] in ^{89,95}Zr and in ^{207}Pb. Using a surface peaked interaction $U_1(r)$ a correct energy splitting could only be obtained with a value $V_1' = 210$ MeV, corresponding to a volume term for the isospin dependent part of the nuclear potential $V_1 = 35$ MeV. This value is in good agreement with the ones deduced from binding energies systematics of hole states in heavy nuclei.[41] We would like to point out, however, that this result is inconsistent with the strength $V_1 = 25$ MeV deduced from elastic scattering and charge exchange reaction analysis.[38] It would also lead to larger discrepancies for the spectroscopic strengths of the low-lying neutron and proton-hole states.

In conclusion, a number of new hole-analog states have been observed in the Sn isotopes. Their identifications are based on their excitation energies and corresponding Coulomb displacement energies (see Table IX), l transfers and spectroscopic strengths, as compared to their parent states. The detailed DWBA analysis of such deeply bound levels has confirmed the inadequacy of the SE procedure in reproducing their spectroscopic strengths. The use of the CC calculations, although leading to a reasonable basic description of such states, cannot explain the energy splitting between the $T_<$ and $T_>$ components for high isospin levels ($T_0 \gtrsim 6$). This result can be tentatively explained by our lack of knowledge concerning the actual form and strength of the isospin dependent part in the nuclear potential for heavy nuclei. According to theoretical descriptions of heavy nuclei,[43] it should include both volume and surface terms. A systematic study of the influence of a volume term in heavy nuclei should be undertaken in order to clarify this question. Additional effects, due to matching conditions or to contributions to the cross section from the high density of $T_<$ unbound states which are not explicitly included in the reaction mechanism, have also to be considered in the analysis of the strength of the analog pairs in heavy nuclei.

VII. SUMMARY

The present work, performed with good energy resolution (38 keV) as compared to previous (^{3}He,α) studies, allows the observation of a number of new features for both the valence and the inner-hole states in the ^{111,115}Sn and ^{119}Sn isotopes.

TABLE IX. Coulomb displacement energies for analog states in Sn isotopes.

Analog pair	E_x (IAS) (keV)	E_x (parent) (keV)	ΔE_c (keV) Exp.	Calc.
^{115}In-^{115}Sn	13 260	0	13 560 ± 30	
	13 630	340	13 580 ± 30	
	13 890	600	13 590 ± 30	13 565 ± 40
	14 330	1040	13 570 ± 30	
	14 760	1480	13 590 ± 30	
	14 930	1670	13 540 ± 30	
^{111}In-^{111}Sn	10 470	0	13 720 ± 30	
	11 060	590	13 710 ± 30	13 735 ± 40
	11 340	870	13 690 ± 30	
^{119}In-^{119}Sn	14 980	0	13 425 ± 30	
	15 340	315	13 470 ± 30	
	15 630	610	13 465 ± 30	13 400 ± 40
	16 100	1050	13 495 ± 40	
	16 470	1450	13 465 ± 40	

[a] The excitation energies from the parent states in In isotopes are from Refs. 31, 32, and 33.
[b] The Coulomb displacement energies were calculated using the semi-empirical formula (Ref. 42) $\Delta E_c = 1430\ (\bar{Z}/A^{1/3}) - 992$, where $\bar{Z}$ is the average charge of the analog pair.

In the intermediate excitation energy region, new states or groups of levels with $l=4$ and $l=5$ angular momentum transfers have been populated in ^{115}Sn. These levels correspond to the fragmentation of the $1h_{11/2}$ and $1g_{7/2}$ valence orbitals and have been explained in the framework of a weak-coupling model. Both the shape and the magnitude of the cross sections for such levels are rather well reproduced by coupled-channels reaction calculations, using the wave functions determined from the model. The one-hole components, even small, generally dominate the observed cross sections. This model also accounts for the population of an "anomalous" $l=6$ transition corresponding to a $J^\pi = \frac{11}{2}^+$ state with collective character. A satisfactory explanation of the $l=3$ ($\frac{5}{2}^-, \frac{7}{2}^-$), $l=4$ ($\frac{9}{2}^+$), and $l=1$ transitions is also obtained if one includes in the calculation the $1g_{9/2}$, $2p$, and $1f$ inner-hole orbitals located above 4 MeV.

In the two other isotopes, new peaks and structures with large l values ($l>2$) are also evidenced in this work. We would like to point out the striking differences observed in the intermediate energy region (~1 to 3.6 MeV) in these two isotopes. This behavior reflects, in the framework of the weak-coupling scheme, the change of the neutron quasihole energies with increasing mass number, while the energies of the collective 2_1^+ and 3_1^- remain comparatively independent of A.

In the $1g_{9/2}$ inner-hole region, the experiment has established the existence of "fine structure" in the three isotopes, in agreement with the results of our previous (d, t) study on ^{116}Sn. The modification of the fine structure aspect of this inner-hole strength with the mass number is clearly demonstrated. A limited number of strongly excited narrow states around 4.2 MeV in ^{111}Sn are populated, whereas in ^{119}Sn the fine structure is less pronounced and the small peaks are observed on an underlying broad bump. The $(^3\mathrm{He}, \alpha)$ reaction leads to a more reliable measurement of the $1g_{9/2}$ strength, since the lower l components ($2p$) are strongly reduced in the bump region. These $l=1$ components, however, appear on each side (A and C) of the main structure B, which contains pure $l=4$ states. A very large spreading of the $l=1$ strength up to ~11 MeV is suggested by this experiment.

The measured strength in the fine structure region (A + B + C) is equal to 62%, 43%, and 28% of the total strength in the ^{111,115,119}Sn isotopes. No more fine structure is observed above these regions and the cross section decreases smoothly up to the IAS region. The theoretical calculations are able to reproduce neither the observed fragmentation nor the deduced spectroscopic strengths.

The corresponding $T_>$ inner-hole components with large isospins ($T_> = \frac{13}{2}$, $\frac{17}{2}$, and $\frac{21}{2}$ in, respectively, ^{111}Sn, ^{115}Sn, and ^{119}Sn) are nicely resolved. The analysis of such $T_>$ components of inner-hole states using Lane's form factor is compared to the standard SE procedure. Both calculations reproduce very well the shapes of the experimental angular distributions, but lead to rather different

results for the spectroscopic strengths. The Lane coupled-channels approach applied in a consistent way to both the parent proton-hole and the $T_<$ neutron-hole levels reveals a number of contradictory results. The analysis demonstrates that for analog states with large isospin a more refined description of the isospin dependent part of the nuclear potential is needed in order to describe the strength of the parent, analog, and $T_<$ states in heavy nuclei.

ACKNOWLEDGMENT

The authors would like to thank Mrs. Doury for the preparation of the targets, the tandem crew for the good running of the accelerator, and K. Heyde, P. D. Kunz, and E. Rost for fruitful discussions.

*Permanent address: Lebanese University, Faculty of Sciences, Hadat-Beyrouth, Liban.

[1]G. Berrier-Ronsin, G. Duhamel, E. Gerlic, J. Kalifa, H. Langevin-Joliot, G. Rotbard, M. Vergnes, J. Vernotte, and K. K. Seth, Phys. Lett. 67B, 16 (1977).
[2]G. Berrier-Ronsin, G. Duhamel, E. Gerlic, J. Kalifa, H. Langevin-Joliot, G. Rotbard, M. Vergnes, J. Vernotte, K. K. Seth, and K. Heyde, Nucl. Phys. A282, 189 (1977).
[3]S. Y. Van der Werf, M. N. Harakeh, L. W. Put, O. Scholten, and R. H. Siemssen, Nucl. Phys. A289, 141 (1977) and references therein.
[4]D. G. Flemming, Orsay Internal Report No. IPNO-PhN-78-22.
[5]M. Sekiguchi, Y. Shida, F. Soga, Y. Hirao, and M. Sakai, Nucl. Phys. A278, 231 (1977).
[6]M. Tanaka, T. Yamagata, K. Iwamoto, S. Kishimoto, B. Saeki, K. Yuasa, T. Fukuda, I. Miura, K. Okada, M. Inoue, and H. Ogata, Phys. Lett. 78B, 221 (1978).
[7]E. Gerlic, J. Källne, H. Langevin-Joliot, J. Van de Wiele, and G. Duhamel, Phys. Lett. 57B, 338 (1975); J. Van de Wiele, E. Gerlic, H. Langevin-Joliot, and G. Duhamel, Nucl. Phys. A297, 61 (1978).
[8]P. D. Kunz, A distorted wave Born approximation computer program, University of Colorado (unpublished).
[9]C. M. Perey and F. G. Perey, Nuclear Data Tables 13, 293 (1974).
[10]S. Galès, E. Hourani, S. Fortier, H. Laurent, J. M. Maison, and J. P. Schapira, Nucl. Phys. A288, 221 (1977); E. Friedland, M. Goldschmidt, C. A. Wiedner, J. L. C. Ford Jr., and S. T. Thornton, *ibid.* A256, 93 (1976).
[11]J. W. Luetzelschwab and J. C. Hafele, Phys. Rev. 180, 1023 (1969).
[12]G. Ch. Madueme, L. Westenberg, L. O. Evardson, and M. Migahad, Phys. Scr. 12, 189 (1975).
[13]D. G. Flemming, F. D. Bechetti, and E. R. Flynn, Los Alamos Internal Report No. LA-UR-79-153.
[14]K. Heyde and P. J. Brussaard, Nucl. Phys. A104, 81 (1967) and references therein.
[15]K. Heyde, private communication.
[16]B. L. Cohen, in *Nuclear Spin Parity Assignments*, edited by N. B. Gove (Academic, New York, 1966), p. 365.
[17]T. Koeling and F. Iachello, Nucl. Phys. A295, 45 (1978).
[18]E. Rost and P. D. Kunz, private communication.
[19]P. E. Cavanagh, C. F. Coleman, A. G. Hardacre, G. A. Gard, and J. F. Turner, Nucl. Phys. A141, 97 (1970).
[20]P. J. Blankert, Thesis, 1979, Free University, Amsterdam.
[21]B. Fogelberg, L. E. de Geer, K. Fransson, and M. af Ugglas, Z. Phys. A276, 381 (1976).
[22]A. I. Vdovin, Ch. Stoyanov, and Chan Zuy Khuong, J.I.N.R., Dubna, 1978, Report No. E4-12012.
[23]Masao Nomura, Prog. Theor. Phys. 55, 622 (1976).
[24]J. M. Moss, D. R. Brown, D. H. Youngblood, C. M. Rozna, and J. D. Bronson, Phys. Rev. C 18, 741 (1978).
[25]J. P. Schiffer, in *Isospin in Nuclear Physics*, edited by D. H. Wilkinson (North-Holland, Amsterdam, 1969), p. 665.
[26]S. Galès, E. Hourani, S. Fortier, H. Laurent, J. M. Maison, and J. P. Schapira, Nucl. Phys. A228, 220 (1977).
[27]R. L. Kozub and D. H. Youngblood, Phys. Rev. C 7, 410 (1973).
[28]S. Galès, Y. El Hage, S. Fortier, H. Laurent, J. M. Maison, and J. P. Schapira, Phys. Rev. C 17, 1308 (1978).
[29]S. Galès, G. M. Crawley, D. Weber, and B. Zwieglinski, Phys. Rev. Lett. 41, 292 (1978).
[30]G. Duhamel, G. Perrin, J. Chauvin, M. Buenerd, E. Gerlic, J. Guillot, J. P. Didelez, H. Langevin-Joliot, and J. Van de Wiele, Phys. Lett. 78B, 213 (1978).
[31]M. Conjeaud, S. Harar, and E. Thuriere, Nucl. Phys. A129, 10 (1969).
[32]W. H. A. Hesselinck, B. R. Kooistra, L. W. Put, R. H. Siemssen, and S. Y. Van der Werf, Nucl. Phys. A226, 229 (1974).
[33]C. V. Weiffenbach and R. Tickle, Phys. Rev. C 3, 1668 (1971).
[34]F. D. Bechetti, W. S. Gray, J. Janëcke, E. R. Sugarbaker, and R. S. Tickle, Nucl. Phys. A271, 77 (1976).
[35]H. Ikegami, T. Yamazaki, S. Morinobu, I. Katayama, M. Fujiwara, Y. Fujita, H. Taketani, M. Adachi, Y. Matsuzaki, M. Mataba, and N. Koori, Osaka University Annual Report, 1977, p. 195.
[36]R. Stock and T. Tamura, Phys. Lett. 22, 304 (1966).
[37]A. M. Lane, in *Isospin in Nuclear Physics*, edited by D. H. Wilkinson (North-Holland, Amsterdam, 1969), p. 511.
[38]G. R. Satchler, in *Isospin in Nuclear Physics*, edited by D. H. Wilkinson (North-Holland, Amsterdam, 1969), p. 391.
[39]M. Beiner and P. Gara, Comput. Phys. Commun. 4, 1 (1972).
[40]S. Fortier, N. M. Rao, E. Hourani, and S. Galès, Nucl. Phys. A311, 324 (1979).
[41]T. Ishimatsu, H. Saito, M. Yambe, T. Awaya, and H. Nomura, Nucl. Phys. A246, 21 (1975).
[42]J. Janëcke, in *Isospin in Nuclear Physics*, edited by D. H. Wilkinson (North-Holland, Amsterdam, 1969), p. 299.
[43]C. B. Dover and Nguyen Van Giai, Nucl. Phys. A190, 373 (1972).